AN EXAMINATION OF ANALYSIS AND OPTIMIZATION PROCEDURES WITHIN A PBSD FRAMEWORK

by

ANDREW COTT

B.S., Kansas State University, 2009

A REPORT

submitted in partial fulfillment of the requirements for the degree

MASTER OF SCIENCE

Department of Architectural Engineering
College of Engineering

KANSAS STATE UNIVERSITY
Manhattan, Kansas

2009

Approved by:

Major Professor
Kimberly Waggle Kramer, P.E.

Abstract

The basic tenets of performance based seismic design (PBSD) are introduced. This includes a description of the underlying philosophy of PBSD, the concept of performance objectives, and a description of hazard levels and performance indicators. After establishing the basis of PBSD, analysis procedures that fit well within the PBSD framework are introduced. These procedures are divided into four basic categories: linear static, linear dynamic, nonlinear static, and nonlinear static. Baseline FEMA requirements are introduced for each category. Each analysis category is then expanded to include a detailed description of and variations on the basic procedure. Finally, optimization procedures that mesh well with a PBSD framework are introduced and described. The optimization discussion focuses first on the solution tools needed to effectively execute a PBSD multi-objective optimization procedure, namely genetic and evolutionary strategies algorithms. Next, multiple options for defining objective functions and constraints are presented to illustrate the versatility of structural optimization. Taken together, this report illustrates the unique aspects of PBSD. As PBSD moves to the forefront of design methodology, the subjects discussed serve to familiarize engineers with the advantages, possibilities, and finer workings of this powerful new design methodology.

Table of Contents

List of Figures

List of Tables

CHAPTER 1 - Introduction

Generally, current code requirement and design practice in the United States is to design structures to a baseline Life Safety level. In the case of building seismic design, the purpose of Life Safety design practice is that while the structure may be rendered unusable by the severity of a seismic event, the occupants of that building will survive. In meeting this United States design practice goal, Life Safety design has been successful: very few human casualties due to seismic collapse have become the norm. Because of the success of Life Safety code design, the prevention of fatalities resulting from building seismic collapse is not the motivating factor behind advancing earthquake design methodology that it once was. Rather, a new concern has arisen: cost.

For the decade that began in 1988 and ended 1997, total estimated earthquake losses were twenty times larger than in the previous thirty years combined. It has been predicted that future single earthquakes may result in losses of $50-100 billion each (Federal Emergency Management Agency [FEMA] 349, 2000). FEMA 349 (2000) notes that this staggering increase in cost is due to several factors: denser population of buildings located in high seismic regions, an aging building stock, and the increasing cost of business interruption. Hamburger (1997) points out that earthquake damage cost figures have reached such high levels as to become "a source of concern to the business, financial, and emergency management communities." Current building codes may succeed in protecting lives, but they do nothing to quantify, control, or even mention building usability after an earthquake. As a result, many to most structures that survive a severe earthquake are no longer able to function as originally intended.

How then, are our current codes insufficient? FEMA 349 (2000) answers this question: "current codes do not" have a system to "evaluate a building's performance after the onset of damage." Instead, current codes "obtain compliance with a minimum safety standard by specifying a design which historically has predicted life safety." Freeman, Paret, Searer, and Irfanoglu (2004) go further, pointing out that prescriptive current codes use pseudo-demands and pseudo-capacities in building design. Pseudo-demands are the result of elastic demands being scaled to approximate inelastic behavior, while pseudo-capacities stem from the use of minimum expected strengths rather than best estimate strengths. Perhaps the simplest reason why current

codes do not have a system to effectively predict and manage structural damage is because predicting and managing structural damage is not the intent of current codes. Their purpose is restricted to the preservation of life safety with little if any provisions made for developing a truly descriptive picture of post-earthquake structural damage conditions.

These and other concerns have led the industry to a new methodology: Performance-Based Seismic Design. The essence of Performance-Based Seismic Design (PBSD) lies in minimizing uncertainty while simultaneously maximizing confidence in predictable building structural damage. In doing so, engineers and owners can succeed in minimizing the risk of costly building damage during a seismic event. In taking the lead in PBSD methodology development, FEMA 349 (2000) has stated that "the basic concept of PBSD is to provide engineers with the capacity to design buildings that will have a predictable and reliable performance in earthquakes." PBSD seeks to extend the reach of design engineers from life safety assurance to damage control and quantification. As a result, engineers can form a more complete picture of the structural response and associated structural damage of a seismic event. This new design philosophy encourages "a design that would achieve, rather than be bounded by, a given performance limit state under a given seismic intensity" (Priestley, 2000). Utilizing new methodologies and tools allows designers and owners to gain greater insight into building response characteristics and make better decisions about how to restrict building damage and minimize cost.

1.1 Performance Objectives

The most apparent departure between current code methods and PBSD is in the selection of a Performance Objective, of which there are four: Collapse Prevention, Life Safety, Immediate Occupancy, and Operational (FEMA 273, 1997). Qualitative descriptions of the four performance levels are included in Table 1.1-1. "A performance objective is the specification of an acceptable level of damage to a building if it experiences an earthquake of a given severity" (FEMA 349, 2000). Inherent in that definition and in the legitimacy of PBSD procedure is the assumption that these qualitative statements can be quantified. Indeed, quantification of damage and hazard is the basis of establishing each of the four performance objectives listed above.

Table 1.1-1 Qualitative Description of Performance Levels

Performance Level	Description
Operational	No permanent drift. Structure substantially retains original strength and stiffness. Minor cracking of facades, partitions, and ceilings as well as structural elements. All systems important to normal operation are functional
Immediate Occupancy	No permanent drift. Structure substantially retains original strength and stiffness. Minor cracking of facades, partitions, and ceilings as well as structural elements. Elevators can be restarted. Fire protection operable.
Life Safety	Some residual strength and stiffness left in all stories. Gravity-load-bearing elements function. No out-of-plane failure of walls or tipping of parapets. Some permanent drift. Damage to partitions. Building may be beyond economical repair.
Collapse Prevention	Little residual stiffness and strength, but load-bearing columns and walls function. Large permanent drifts. Some exits blocked. Infills and unbraced parapets failed or at incipient failure. Building is near collapse.

Source: U.S. Federal Emergency Management Agency. (2000, November). *Prestandard and Commentary for the Seismic Rehabilitation of Buildings, FEMA 356*. Washington, DC: U.S. Government Printing Office.

The pairing of an earthquake hazard level with a structural performance level creates a performance objective. Earthquake hazard is expressed as the probability of exceedance of a certain seismic intensity over a given period of time. For example, earthquake hazard may be stated as 2% probability of exceedance in fifty years – a very severe event – or as 50% probability of exceedance in fifty years – a very mild event. The structural performance level is a measure of structural damage, usually interstory drift. Interstory drift is the most often chosen structural performance level because it is a global response parameter that is well correlated with local response parameters that indicate damage of structural members. In particular, interstory drift has been shown to correlate well with plastic hinge formation which itself is a good indicator of deformation and therefore damage within individual structural members. Drift limits associated with a specific performance objective are unique to each type of lateral force resisting system. Quantitative structural performance levels, based on interstory drift, are included for sample lateral force resisting systems in Table 1.1-2. So, an example of a selected

performance objective may be Immediate Occupancy, which means that the hazard level of concern is an earthquake with 50% probability of exceedance in fifty years and –for a steel moment frame structure – a structural performance level of 0.7% transient interstory drift. The four performance objectives range as stated from worst to best performance, with better performing objectives being designed to less severe earthquakes and smaller drift quantities.

Table 1.1-2 Quantitative Structural Performance Levels by Interstory Drift

	Structural Performance Level		
LFRS	Collapse Prevention	Life Safety	Immediate Occupancy
Steel Moment Frames	5% transient or permanent	2.5% transient; 1% permanent	0.7% transient; negligible permanent
Steel Braced Frames	2% transient or permanent	1.5% transient; 0.5% permanent	0.5% transient; negligible permanent
Concrete Frames	4% transient or permanent	2% transient; 1% permanent	1% transient; negligible permanent

Source: U.S. Federal Emergency Management Agency. (2000, November). *Prestandard and Commentary for the Seismic Rehabilitation of Buildings, FEMA 356*. Washington, DC: U.S. Government Printing Office.

A building may be designed to two or more performance levels. For example, Life Safety may be ensured, and then the building performance expanded to include Immediate Occupancy performance. The variance in suggested seismic hazard that each structural performance level should be designed for necessitates a unique evaluation for each performance objective being sought. It is this facet of PBSD that led Freeman et al. (2004) to describe the methodology as a "performance menu." Clearly, this makes PBSD a powerful tool for making initial design decisions. The engineer, with owners and other stake holders, can make informed, calibrated decisions about the level of risk beyond life safety the owners and other stake holders are willing to accept.

While the performance objectives are certainly a major advancement, a caveat should be kept in mind. A goal of PBSD is to remove a large number of uncertainties from the design and analysis procedure, but uncertainties do still remain. It is therefore inaccurate to say or imply that performance can be predicted in an absolute sense and it is furthermore inaccurate that it is absolutely possible to produce designs that will achieve desired performance objectives (FEMA 350, 2000). Rather, it is more accurate to think of achieving performance objectives in terms of levels of confidence and probability. "Performance objectives are statements of the total

probability that damage experienced by a building in a period of years will be more severe than the desired amount, given our knowledge of the site seismicity. Thus, a performance objective that is stated as 'meeting collapse prevention performance for ground motion with a 2% probability of exceedance in fifty years' should more correctly be stated as being 'less than a 2% chance in fifty years that damage more severe than the collapse prevention level will occur, given the mean definition of seismicity'" (FEMA 350, 2000). Understanding this delineation is important in correctly applying the fundamental PBSD philosophy.

After the targeted level of performance has been selected the next step is to evaluate that performance. Performance evaluation can be done using any of several different types of analysis, each type having its own unique advantages and disadvantages. Results from the selected analytical procedure are then compared to the damage levels of the pertinent performance objective. Then, the designer must make a decision: Have the structural performance levels been satisfied with sufficient confidence? If so, the process has reached completion. If not, parameters of the structure itself may be altered or a different type of analysis may be selected. The different types of analysis range in levels of accuracy, and so perhaps a more rigorous analysis may provide better accuracy and thus better confidence that the selected performance level has been met. In any case, the methodology of PBSD is a flexible one by which goals and methods for achieving those goals can be easily adjusted during the design and analysis process.

PBSD guarantees six advantages: (1) multilevel seismic hazards are considered with an emphasis on the transparency of performance objectives, (2) building performance is guaranteed through limited inelastic deformation in addition to strength and ductility, (3) seismic design is oriented by performance objectives interpreted by engineering parameters performance criteria, (4) an analytical method through which the structural behavior, particularly the nonlinear behavior is rationally obtained, is required, (5) the building will meet the prescribed performance objectives reliably with accepted confidence, and (6) the design will ensure minimum life cycle cost (Xue, Wu, Chen, & Chen, 2008). While FEMA has taken the lead in developing a consistent PBSD methodology, much of the work published by FEMA has been conceptual in nature. A solid framework has been provided, but a fleshing out of that framework such that the full scope of capabilities of PBSD may be realized has yet to be established. The goal of this report is to build on the fundamental framework by showing the many-faceted possibilities of

implementing a PBSD procedure. Structural engineers must evaluate buildings using various analysis procedures, and, based on the system in question, they must work to verify objectives and, where possible, go beyond these objectives by utilizing optimization procedures. All these tasks fit neatly into the fundamental goal of PBSD: creating a more descriptive building design to minimize building damage cost.

CHAPTER 2 - Analysis

The framework established by various FEMA documents defines four basic types of analysis for use in a PBSD procedure: linear static, linear dynamic, nonlinear static, and nonlinear dynamic. Each of these four types have trade-offs relative to the other three. The trade-offs among the various types of analysis procedures revolve around relative levels of uncertainty. Simpler procedures tend to introduce more uncertainty while the reverse tends to be true for more computationally demanding procedures. This point is illustrated by Figure 2-1. Figure 2-1 compares different categories of static procedures to different categories of dynamic procedures. As can be seen, for linear and dynamic procedures that use the same type of structural model, dynamic procedures tend to have lower levels of uncertainty relative to the static procedures. The procedures range in terms of accuracy, level of computational burden, and degree of applicability. The following sections examine each PBSD analysis procedure, including restrictions, method, advantages, disadvantages, and corresponding extensions or modifications.

Figure 2-1 Relative Uncertainty of Analysis Procedures

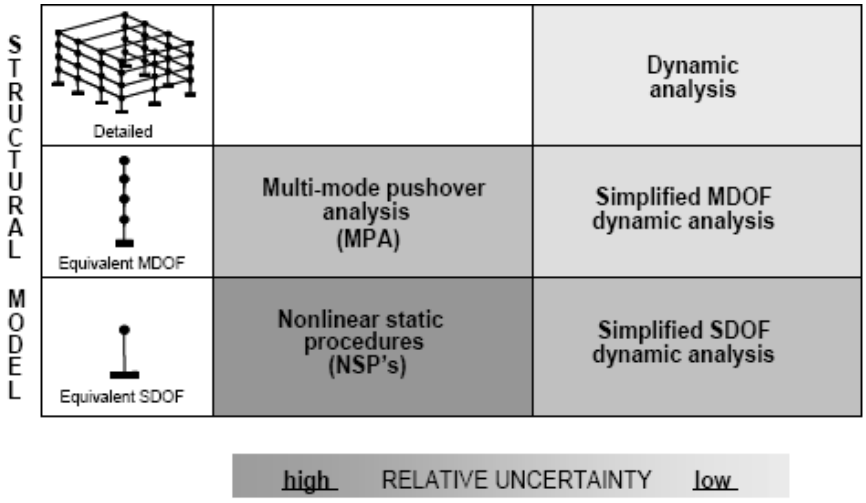

Source: U.S. Federal Emergency Management Agency. (2005, June). *Improvement of Nonlinear Static Seismic Analysis Procedures, FEMA 440*. Washington, DC: U.S. Government Printing Office.

2.1 Linear Static

The linear static procedure for analysis, initially outlined in FEMA 273 (1997) and updated in FEMA 356 (2000), is a simple procedure. Due to its simplicity, its implementation is

subject to numerous restrictions and its results are generally a very rough approximation of actual building behavior. This is because the simplicity of a linear static procedure is rooted in the fact that numerous approximations and assumptions are made that are only valid for a narrow range of building geometries and seismic hazards.

This procedure in general hews closely to the Equivalent Lateral Force Procedure defined by the American Society of Civil Engineers (ASCE) standard, ASCE 7-05 *Minimum Design Loads for Buildings and Other Structures.* Particular differences can be found in determining the seismic base shear of a structure (termed pseudo lateral load by FEMA) and in the unique component restrictions imposed by the FEMA methodology.

Global building restrictions defined in FEMA 356 (2000) are very similar to ASCE 7 restrictions. The linear static procedure, in the PBSD sense, may not be used to analyze a structure for performance evaluation if any of the following are true: building height exceeds 100 feet, the ratio of horizontal dimensions at adjacent stories exceeds 1.4, severe torsional irregularities (as defined in ASCE 7-05) exist, severe vertical mass or stiffness irregularities (as per ASCE 7-05) exist, or the building has a non-orthogonal lateral force resisting system. Therefore, it is a procedure for rigid structures without any horizontal or vertical irregularities in which the load path and performance of the LFRS of the structure are somewhat predictable. It should be pointed out that FEMA documents do not directly reference the ASCE 7-05 standard, rather the parallel has been included here to ground the requirements in a more commonly used reference.

FEMA 273 (1997) and 356 (2000) are unique in their inclusion of individual component checks. For each of the various components of a structure's primary lateral force resisting system (LFRS), a demand-capacity ratio (DCR) must be computed. DCRs must be computed for every structural response action (axial, bending, etc.) and for every component and is defined as the ratio of the expected force to expected strength. Expected force is the maximum combination of vertical gravity and horizontal earthquake loading. The effective vertical gravity loading used includes dead, live, and snow load, where live and snow loading are appropriately reduced based on FEMA 273 (1997) and FEMA 356 (2000) provisions. Expected strength is the calculated minimum limit state strength for a particular component under a particular action. The values of the DCRs are used to gage the applicability of the linear static procedure. For a component where all DCRs are less than or equal to unity the component can be expected to respond

elastically. For a component where all DCRs are less than two the linear procedure is applicable. If some computed DCRs exceed two, then linear procedures should not be used if any of the discontinuities already mentioned exist (FEMA 356, 2000).

The method for determining the total pseudo lateral load for a structure consists of multiplying the effective seismic weight by the response spectrum acceleration and three modification factors: C_1, C_2, and C_3. The modification factors C_1, C_2, and C_3 are used to modify the pseudo load by approximating the effects of inelastic behavior for an elastic structure, by approximating the effects of stiffness degradation and strength deterioration, and by approximating increased displacements due to dynamic P-Δ effects, respectively. By implementing the modification factors, the pseudo lateral load, V, is taken to represent a simulation of the actual force on an inelastic system on what is in reality designed as an elastic system. The modification factors depend on the fundamental period of the LFRS, which is determined in the same manner as given in the ASCE 7-05 standard. The vertical distribution of the pseudo lateral force over the height of the structure is also the same as in the ASCE 7-05.

Clearly, the linear static procedure is a truly approximate method. Inelasticity is not considered directly and the procedure provides only approximations of actual behavior, forces, and displacements. Additionally, a static load is applied to the structure which attempts to simulate a dynamic response. This procedure has significant limitations on its application. The procedure is not capable of giving a truly descriptive picture of building action during earthquake loading and should be used only for very regular, rigid structures expected to respond almost completely elastically. Though, if the requisite conditions are met, the procedure does have the advantage of being very computationally simple. Under the proper conditions, the procedure does give a good prediction for interstory drift, though it is likely that calculated internal forces will exceed the internal forces seen by the actual structure. The former observation is explained by the fact that the three modification factors were calibrated and introduced for the express purpose of ensuring this outcome. The latter observation is due to the fact that the modification for anticipated nonlinear behavior does not extend to the individual members in the linear elastic model and the procedure does not appropriately account for force redistribution due to yielding which overestimates element stiffness and therefore internal element forces. For more complex structures under more severe loading, more robust analysis tools are needed.

2.2 Linear Dynamic

Linear dynamic procedures are constrained in their use by the same requirements outlined for linear static procedures. Also, all output – whether deformations or forces – found using a linear dynamic procedure must be multiplied by the same three modification factors, C_1, C_2, and C_3, discussed for linear static procedures. It is through these factors that inelastic behavior can be approximated from a linear-elastic model. Implementing these approximations, when the appropriate constraints are met, is advantageous due to the significant reduction in computational effort seen in linear procedures compared to nonlinear procedures.

The linear dynamic procedure may be executed through either of two different methods: the Response Spectrum Method (RSM) or Time History Analysis (THA). An RSM procedure consists of first executing a modal spectral analysis for the linear-elastic response of the structure in question. Then, the peak member forces, displacements, story forces, story shears, and base reactions for each significantly participating mode are combined using either the square-root-sum-of-squares (SSRS) rule or the complete quadratic combination (CQC) rule. FEMA 273 (1997) and FEMA 356 (2000) both define "significantly participating modes" as those modes that are sufficient to capture 90% of the participating mass in each of the building's principal horizontal directions. The RSM is similar to the Modal Response Spectrum analysis outlined in ASCE 7-05.

Time History Analyses are executed by making a time step by time step evaluation of building response using discretized recorded or synthetic earthquake records as the base model input. Specific requirements are made by FEMA 273 (1997) and FEMA 356 (2000) concerning the type and quantity of earthquake records used. At least three recorded events or data sets must be used to sufficiently execute a THA. For cases where more than seven records are used, the average value of each response parameter may be used to determine design acceptability. For cases where three to seven records are used, the maximum value of each response parameter must be used to determine design acceptability.

Linear dynamic procedures are expected to give results similar to the quality of results given by linear static procedures. That is, interstory drift values given by a linear dynamic analysis are good approximations of actual building response while internal forces are expected to be overestimated. These observations may be explained by the same reasoning given for linear static procedures. A linear dynamic procedure is narrowly advantageous relative to a

linear static procedure in that a linear dynamic procedure directly accounts for the stiffness and mass distribution of a structure. Because of this, linear dynamic procedures generally introduce less uncertainty than linear static procedures (FEMA 356, 2000).

2.3 Nonlinear Static

Nonlinear static procedures are simplified procedures, though to a lesser degree than linear static or dynamic procedures, and as such are more powerful and accurate tools for performance objective evaluation. Nonlinear static procedures eliminate more uncertainty than either of the linear procedures. Nonlinear static procedures reduce uncertainty by directly including material nonlinearity, while linear procedures do not. The basic procedure of a nonlinear static procedure (or pushover analysis, as it is sometimes called) is to apply increasing monotonic lateral loads to an equivalent single degree of freedom (SDOF) system that approximates an actual multi-degree of freedom (MDOF) system. Loads are increased until one of two things happens: either the structural model collapses or a predefined target displacement is reached. The results, usually in terms of total base shear and lateral roof displacement, are plotted to form a pushover curve, an example of which is included in Figure 2.3-1. This process estimates global displacement demand (by measuring lateral roof displacement) which is then used to determine interstory drift and member forces by relating the global displacement to a capacity curve (FEMA 440, 2005). Ground motions are represented by response spectra and nonlinear static procedures generally rely on the structure's first mode of vibration.

Figure 2.3-1 Sample Pushover Curves

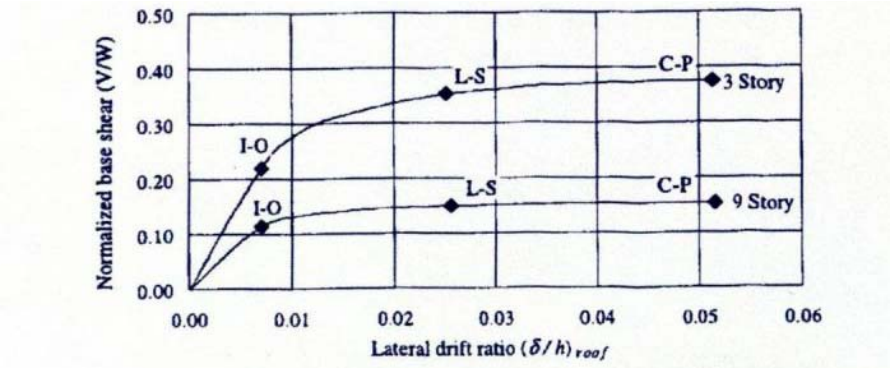

Source: Hasan, R., & Xu, L., & Grierson, D. (2002). Push-over analysis for performance-based seismic design. *Computers and Structures, 80,* 2483-2493.

FEMA 273 (1997) and FEMA 356 (2000) place limits on the applicability of the nonlinear static procedure. A fundamental assumption of most nonlinear static procedures is that

the first mode of vibration is dominant and thus is the only mode that need be considered. This observation has been empirically justified for structures with shorter natural periods and is widely recognized in engineering practice. The FEMA limitations directly check this assumption. A check for significant higher mode contribution is a two step process. First a modal response spectrum analysis, using enough modes to capture 90% of mass participation in each principal horizontal direction, is performed. Next, a second modal response spectrum analysis is performed that considers only the first mode. Finally, a comparison is made between the first and second modal response spectrum analyses. If the shear in any story from the first analysis is greater than 130% of the second analysis, then the single mode nonlinear static procedure should not be used (FEMA 356, 2000). This stipulation is imposed to verify the assumption that the first mode of vibration is sufficiently dominant such that it can be judged to represent the total response of the structure. Otherwise, the nonlinear static procedure is a good method for analyzing structures that do not conform to the various restrictions imposed upon the two linear methods.

The previous information is the basic considerations applicable to most nonlinear static procedures. However, many different variations and extensions upon the material already presented exist. The following sections are a deeper exploration into the intricacies of several nonlinear static procedure variations and enhancements: coefficient method, capacity spectrum method, pushover using matrix structural analysis, and multimode methods.

2.3.1 Coefficient Method

Originally published in FEMA 273 (1997) and subsequently repeated in FEMA 356 (2000) and FEMA 350 (2000), a suggestion for determining target displacement has been made. Target displacement is the lateral roof displacement at which the pushover analysis is terminated. The target displacement is a computed estimation of the maximum displacement due to dynamic forces that the structure is likely to undergo. In this way, the static analysis is more closely tied to the dynamic loading reality. While the coefficient method has gained traction in some of the literature, it is not the only way to determine a target displacement, δ_t. In fact, FEMA documents allow that the target displacement may be determined from any procedure that accounts for nonlinear effects on displacement amplitude. The variation in the determination of target displacement is often the delineating characteristic between different nonlinear static procedures.

These variations are addressed in subsequent sections. This being said, the coefficient method for determining target displacement is as follows (FEMA 356, 2000):

$$\delta_t = C_0 C_1 C_2 C_3 S_a \frac{T_e^2}{4\pi^2} g \qquad \text{Equation 2.3.1-1}$$

Where S_a is the response spectrum acceleration, T_e is the effective fundamental period of the building, C_0 is a modification factor to relate spectral displacement and likely building roof displacement, C_1 is a modification factor to relate expected maximum inelastic displacements to displacements calculated for linear force response, C_2 is a modification factor to represent the effect of hysteresis shape on the maximum displacement response, and C_3 is a modification factor to represent increased displacements due to dynamic P-Δ effects. The effective fundamental period is based on the elastic fundamental natural period, determined from elastic dynamic analysis, and adjusted based on the discrepancy between the structure's actual elastic lateral stiffness and the structure's effective lateral stiffness. The effective lateral stiffness is determined statically by applying a base shear that is approximately 60% of the yield strength of the structure. The approximations made in determining the structure's effective fundamental period are important in maintaining the computational attractiveness of a nonlinear static procedure. The elastic fundamental period of a structure is altered in an approximate fashion to spare the engineer the computational burden associated with determining the true period of vibration that changes continually under dynamic loading conditions due to progressive yielding within the structure.

Equation 2.3.1-1 is full of adjustment factors, similar to linear procedures. While perhaps being computationally attractive, the target displacement determination procedure of FEMA 273 (1997) is not reassuring in our goal to limit uncertainty.

This procedure has been termed the Coefficient Method and, due to its heavy reliance on approximation and estimation, it received an update in FEMA 440 (2005). The four modification factors were adjusted in their computation as well as in their meaning. C_0 has been adjusted to relate the displacement for an equivalent SDOF system to the roof displacement of the building MDOF system. C_0's computational method has not changed. C_1 is now a modification factor to relate the expected maximum displacements of an inelastic SDOF oscillator with elastic-perfectly-plastic hysteresis properties to displacements calculated for the linear elastic response. The procedure to compute C_1 has been improved. While in previous FEMA editions C_2 represented degradation in both strength and stiffness of a hysteresis type, it

now represents only the stiffness degradation. C_2 is still computed just as in FEMA 273 (1997) and FEMA 356 (2000). C_3 has not been changed either in its definition or computation. Comparative studies published in FEMA 440 (2005) show that these changes have significantly improved the accuracy of the Coefficient Method.

2.3.2 Capacity Spectrum Method

The capacity spectrum method is another nonlinear static procedure developed by the Applied Technology Council (ATC) and published in ATC-40 (1996). This method focuses on developing another procedure for determining the target displacement, though ATC-40 adopts the term demand displacement. The terms "demand displacement" and "target displacement" are synonymous. The capacity spectrum method is a graphical method whereby two curves, one representing structural capacity and the other describing structural demand, are drawn in the Acceleration-Displacement Response Spectra (ADRS) format. The intersection of these curves is termed the performance point. The performance point is interpreted as the point at which the capacity of the structure is equal to the seismic demands being imposed on the structure. The analytical output at this point is used to evaluate performance relative to the stated performance objective. The displacement at the performance point, the demand displacement, is compared to the structural performance level dictated by the adopted performance objective. The procedure of the capacity spectrum method focuses on appropriately evaluating the respective curves.

The capacity spectrum method begins by developing a pushover curve where total base shear, V, is plotted against roof level lateral displacement, Δ. Because the pushover curve is not the final product of the capacity spectrum method, the pushover analysis procedure for this method is not terminated at a target displacement nor are the lateral load forces necessarily based on ground motions the structure is likely to experience. Instead, the pushover procedure here is continued until structural collapse. The lateral forces applied are essentially arbitrary in the sense that they do not necessarily need to be based on site seismicity but rather need only be applied over the height of the building in an appropriate fashion and have significant total magnitude to push the structure all the way to collapse. The vertical distribution of forces should be based on the ASCE 7-05 method and the sum of these individual story forces is the total base shear. The pushover analysis can be done using commercial nonlinear software (like DRAIN-2DX) or via a matrix structural analysis method where the structural stiffness matrix is updated

at each load step to reflect the inelastic behavior of the structure (one such method is described below). In either case, a curve is developed that tracks total applied base shear against total roof level displacement until collapse.

In order to plot demand and capacity simultaneously in the same coordinate plane, the pushover curve must be converted to a capacity spectrum curve. Unlike the pushover curve, the capacity spectrum curve is plotted in terms of spectral acceleration (S_a) and spectral displacement (S_d) which is the defining characteristic of the ADRS format. The curve transformation is achieved by calculating two indices: the modal participation factor for the first natural mode, PF_1, and the modal mass coefficient for the first natural mode, α_1 (ATC-40, 1996). The modal participation factor and the modal mass coefficient depend on the mass and modal amplitude of the first mode at each level of the structure and are given by the relationships:

$$PF_1 = \left[\frac{\sum_{i=1}^{N} (w_i \phi_{i1}) / g}{\sum_{i=1}^{N} (w_i \phi_{i1}^2) / g} \right]$$

Equation 2.3.2-1

$$\alpha_1 = \frac{\left[\sum_{i=1}^{N} (w_i \phi_{i1}) / g \right]^2}{\left[\sum_{i=1}^{N} w_i / g \right] \left[\sum_{i=1}^{N} (w_i \phi_{i1}^2) / g \right]}$$

Equation 2.3.2-2

where φ_{i1} is the modal amplitude of the first mode at level i. The modal participation factor and modal mass coefficient vary according to the relative interstory displacements over the height of the building. The modal mass coefficient increases as relative interstory displacements over the height of the structure become more uniform while the modal participation factor decreases for the same condition (ATC-40, 1996).

ATC-40 (1996) also offers means for estimating the mode shape and modal amplitude, φ. Using any reasonable vertical distribution of forces based on a base shear, V, (the base shear and resulting vertical distribution could be chosen from a single point on the pushover curve, for example) deflections are computed for each story of the structure and then divided by the roof deflection, this value is φ. Next, a new set of story forces is applied. The new force set is

proportional to the weight times the modal amplitude at a given level divided by the total for all levels of the weight times the modal amplitude for each level. Deflections at each story are computed for the new force distribution and again each deflection is divided by the roof deflection. This process is continued until the modal amplitudes converge.

Each individual point on the initial pushover curve, (Δ_i,V_i), corresponds to an individual point on the capacity spectrum curve, (S_{di}, S_{ai}). The transformation is made by utilizing the modal participation factor and modal mass coefficient already calculated and the following relationships (ATC-40, 1996):

$$S_a = \frac{V/W}{\alpha_1} \qquad \text{Equation 2.3.2-3}$$

$$S_d = \frac{\Delta_{roof}}{PF_1 \varphi_{roof,1}} \qquad \text{Equation 2.3.2-4}$$

The pushover curve converted to the ADRS format defines the capacity spectrum.

As mentioned previously, the forces used in the development of the initial pushover curve are essentially arbitrary. This means that both the pushover curve and the capacity spectrum curve are in no way related to the anticipated ground motion at the building site. This obvious discrepancy is compensated for by introducing the demand spectrum. The demand and capacity spectrum curves are essentially independent entities until they are plotted together. The independent development of the two curves allows for parallel computation of each curve which promotes efficiency in the analysis process. Any changes made to either the demand or capacity curve does not affect the other which helps the engineer avoid extensive revisions as the process matures. The demand spectrum is, again, plotted in the ADRS format in terms of spectral acceleration and spectral displacement. Developing the demand spectrum curve has two steps. The first is to transform the more typical elastic design spectrum from acceleration against period coordinates to ADRS coordinates, and the second is to convert the ADRS elastic response spectrum to an ADRS reduced inelastic response spectrum.

Just as the pushover curve was transformed on a point by point basis using simple formulas, so the acceleration versus period response format can be transformed into an ADRS format. The following equation is used (ATC-40, 1996):

$$S_d = \frac{S_a T^2}{4\pi^2} \qquad \text{Equation 2.3.2-5}$$

By executing this equation for each point on the typical response spectrum, (T_i,S_{ai}), a new point for the ADRS response spectrum, (S_d,S_a), is created. In this way the elastic 5%-damped spectral

acceleration versus period curve is converted to an elastic 5%-damped ADRS curve (ATC-40, 1996). A particularly unique characteristic of this new response spectrum curve lies in the fact that any radial straight line drawn outward from the origin represents a curve of constant 5%-damped natural period (Equation 2.3.2-5 can be easily rearranged to give period values). This is notable in that it helps to verify an underlying basis of nonlinear structural analysis. It is well known that structures deforming inelastically will experience a reduction of stiffness and thus a lengthening of the damped natural period. Superimposing the capacity spectrum curve onto the ADRS response curve, when the capacity spectrum curve indicates post-yielding behavior (by strong rightward motion) the capacity curve is also simultaneously crossing into regions of larger natural period (ATC-40, 1996). This is a good confirmation of the efficacy of this procedure.

Finally, the ADRS 5%-damped elastic response spectrum curve is converted into a reduced inelastic response spectrum curve by using the spectral reduction method. The damping experienced by a structure deforming inelastically is a combination of viscous and hysteretic damping. The area contained within the hysteresis loops formed when base shear is plotted against displacement is directly related to the quantity of hysteretic damping. By transforming the total damping in a structure from a combination of hysteretic and viscous damping to equivalent viscous damping only, a reduced demand spectrum curve can be created. Methods for translating hysteretic damping into total equivalent viscous damping are available in the literature, including from Chopra (2007).

The equivalent viscous damping can then be used to develop relationships that estimate spectral reduction factors. These relationships were developed by Newmark and Hall (1982). ATC-40 (1996) provides numerous references, including equations and tabulated values, to aid in the process of determining spectral reduction factors that are used to reduce the elastic response spectrum curve. The final result is a demand spectrum with damping greater than 5% of critical damping. Sample capacity spectrum and demand spectrum curves are shown in Figure 2.3.2-1.

Figure 2.3.2-1 Sample Capacity and Demand Curves

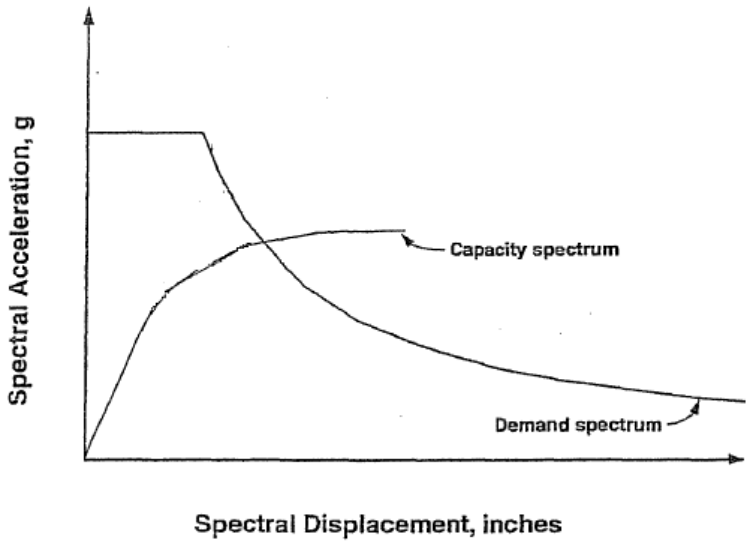

Source: Applied Technology Council. *Seismic Evaluation and Retrofit of Concrete Buildings*, ATC-40, Redwood City, CA, 1996.

With the demand and capacity spectra curves developed, the performance point can be established. The intersection of the curves covers the discrepancy concerning appropriate ground motion expressed earlier. The demand spectrum curve developed in any given analysis procedure will be indicative of the performance objective selected because the ground motion with a probability of exceedance defined by the performance objective is used in the demand spectrum development process. Establishing the performance point is an iterative process and is described by the following.

Identifying the performance point requires several steps. First, the capacity spectrum curve is plotted against the ADRS unreduced response spectrum. A trial intersection point is selected by continuing the linear part of the capacity spectrum curve until it reaches the unreduced 5%-damped response spectrum curve, at which point one draws a line straight back down to the capacity spectrum curve, this is the trial performance point. Next, the demand spectrum curve is also drawn. Then, the designer must determine if the demand spectrum intersects the capacity spectrum at the trial point or if the displacement at which the demand spectrum intersects the capacity spectrum is within an acceptable tolerance of the trial displacement. The acceptable tolerance defined by ATC-40 (1996) is for the actual displacement at intersection to be within 5% of the trial displacement. The 5% tolerance is defined such that the procedure will return reasonably good results while simultaneously lessening the computational burden associated with multiple iterations. If the acceptable tolerance is not met,

a new trial point must be selected and the process repeated. If the acceptable tolerance is met, then the trial performance point is the actual performance point and the displacement ordinate of the performance point is the maximum displacement expected for the demand earthquake (ATC-40, 1996). For performance objective verification, the structural response parameters associated with the maximum expected displacement can be computed and compared to the structural performance level limits established by the performance objective.

As with the coefficient method, the capacity spectrum was reviewed and improved by FEMA 440 (2005). The essential procedure remains the same, but more accurate procedures for determining the equivalent damping and equivalent viscous damping are presented. The result of these modifications were that the coefficient method and the capacity spectrum method now reliably produce equivalent results and, by checking coefficient method and capacity spectrum results against nonlinear time history analysis results, it was found that the two nonlinear static procedures produce reliably good estimates of nonlinear building behavior during seismic events (FEMA 440, 2005).

2.3.3 Pushover Using Matrix Structural Analysis

For a nonlinear static procedure to be truly effective, an ability to detect and trace the emergence of nonlinear behavior in a structure is critical. As a structure is pushed ever closer to collapse, nonlinear behavior propagates and spreads throughout the building in the form of plastic hinges. Missing these developments would pose a serious limitation to the capability of nonlinear static procedures to effectively predict structural damage and describe post-yielding behavior. Detecting and tracing plasticity in a structure can be done by using a nonlinear finite element at the presumed point of yielding or by iteration and reconfiguration within a matrix structural analysis process.

Hasan, Xu, and Grierson (2002) developed a method to detect and trace plasticity through the implementation of a continuous nonlinear post-elastic material model. Their method uses iteration and reconfiguration within a matrix structural analysis process.

Hasan et al. (2002) begin by identifying potential plastic hinge sections and modeling them as pseudo semi-rigid connections. Each moment-connection is described by a linear spring that is quantified by a dimensionless rigidity factor, r. The rigidity factor introduced is defined by the equation (Hasan et al., 2002):

$$r_i = 1/(1 + 3EI/R_iL)$$ Equation 2.3.3-1

where R_i is the rotational stiffness of the connection (for each beam-column member i=1,2). The nondimensional rigidity factor, r_i, is a ratio of the end rotation of a member and the combined rotation of the member and the connection. The rigidity factor takes values in the range of zero to unity while the rotational stiffness varies from one to infinity. Rotational stiffness of infinity translates as a connection being perfectly rigid and completely preserving continuity of elastic deformation. Zero rotational stiffness is the opposite, meaning that the connection is perfectly pinned and permits discontinuity of elastic deformation.

An elastic stiffness matrix to define first-order elastic and second-order geometric properties is given as (Hasan et al., 2002):

$$\boldsymbol{K} = \boldsymbol{K_e C_e} + \boldsymbol{K_g C_g}\mathbf{K}$$ Equation 2.3.3-2

where $\mathbf{C_e}$ and $\mathbf{C_g}$ are correction matrices based on values of the rigidity factor at each end of the member.

Next, a procedure for evaluating post-yielding behavior must be employed. This is done by utilizing a moment-curvature relation. The moment-curvature is developed by stating moment as a function of curvature and equating the function to the yielding moment plus a quantity that accounts for plastic moment, yielding moment, plastic curvature, and curvature for the post yield point in question. The relation developed is (Hasan et al., 2002):

$$M(\varphi) = M_y + \sqrt{(M_p - M_y)^2 - \big((M_p - M_y)(\varphi - \varphi_p)/\varphi_p\big)^2}$$ Equation 2.3.3-3

Differentiating the standard moment-curvature expression with respect to curvature, the rate of post-elastic flexural stiffness degradation, $dM/d\varphi$, is defined. Hasan et al. (2002) found in this new expression sufficient mathematical similarity with the rigidity factor defined previously to conclude that:

$$p = 1/(1 + (3EI/(dM/d\varphi)L)$$ Equation 2.3.3-4

where p is the plasticity factor. The equation was arrived at by merely replacing R in the rigidity factor expression with the rate of flexural stiffness degradation. The plasticity factor is used as a single parameter to measure the stiffness degradation of a connection. The plasticity factor varies in value between zero and unity, zero being completely elastic and unity being perfectly plastic. Finally, the plasticity factor replaces the rigidity factor in the correction matrices mentioned previously. In this way, the structural stiffness matrix is continually revised

throughout the load-increment procedure to include the effects of post-elastic flexural behavior. At each new load step, $dM/d\varphi$ is held constant at the beginning of the step. As the new load increment is applied the moment at each connection is calculated and evaluated to check for a post-yielding quantity. If the computed moment exceeds the yielding moment, a new moment value is computed using the moment-curvature relationship mentioned above. On the basis of the new moment value a new curvature value is computed and on the basis of these values a new $dM/d\varphi$ and subsequently p value is calculated. The $dM/d\varphi$ and p values are used at the beginning of the next load increment. This process is continued for each successive load increment until either the target displacement is reached or the structure collapses, which is signified by a singular structural stiffness matrix (Hasan et al., 2002).

Rather than adopting a method for computing target displacement Hasan et al. (2002) utilize directly the structural performance level associated with the desired performance objective. Thus, unless collapse occurs first, the analysis procedure is terminated when the allowable drift limitation given by FEMA for the desired performance objective is reached. The global displacement of the pushover procedure is measured from the roof of the structure.

To set an appropriate load increment for the analysis, an arbitrarily small spectral acceleration is chosen, in this case $S_a = 0.0008g$. This arbitrary acceleration is multiplied by actual effective weights to give a total base shear, V. The total base shear is then distributed over the height of the structure using the same method given for the Equivalent Lateral Force Procedure in the ASCE 7-05. The value $C_{vx}V$ for each floor is used as the load increment, ΔF, for each individual floor throughout the pushover procedure.

From this procedure, total base shears can be calculated from roof displacement limits at each performance objective, actual maximum tolerable spectral accelerations can be determined from the total base shears for each performance level, any response quantity can be extracted from the matrix procedure, the occurrence and magnitude of nonlinear behavior can be tracked at each connection in the structure, and pushover curves can be constructed.

Hasan et al. (2002) developed a computationally attractive and accurate procedure for evaluating a structure using nonlinear static analysis within a matrix structural analysis approach. The method upholds the importance of nonlinear behavior detection and succeeds – by tracking connection plastification – in developing a detailed picture of post-yield structural performance in the event of an earthquake.

2.3.4Multimode Methods

The nonlinear static procedures discussed so far are effective, computationally attractive methods for analyzing low and mid-rise structures. Because each method described focuses exclusively on the fundamental mode of vibration, they are accurate only for structures with a period of roughly one second or less. Inaccuracy for buildings with longer natural periods of vibration results from the assumption that the first mode of vibration is the governing mode for the structure's behavior. Clearly, this places a limit on the usability of these methods for buildings roughly over 100 feet in height. To overcome this limitation, work has been done to establish an accurate, computationally accessible and attractive method to incorporate multiple modes into a single nonlinear static procedure and thereby extend the use of this method to a larger number of structures. Two different multimode nonlinear static procedures are presented.

2.3.4.1 Force-Based Method

The first multimode method to be examined begins with a notable departure from the nonlinear static procedures described previously: it is force-based. The procedure developed by Grierson, Gong, and Xu (2006) adopts a force-controlled rather than displacement-controlled pushover analysis. This means that rather than terminating the analysis at a given target displacement, the analysis ends at a target level of seismic base shear. The authors adopt an incremental load step method, also known as the Euler method. The Euler method is a single step method in the sense that the increment of unknown displacements can be determined in a single step using an incremental known load and a weighted stiffness quantity that is representative of an entire load increment. The load increment is defined as (McGuire, Gallagher, & Ziemian, 2000):

$$[\boldsymbol{dP}_i] = d\lambda_i[\boldsymbol{P}_{ref}] \qquad \text{Equation 2.3.4.1-1}$$

where $[\boldsymbol{P}_{ref}]$ is a total reference load and $d\lambda_i$ is a load ratio. The quantity $d\lambda_i$ is critical in maintaining accuracy throughout the procedure. For the first load step, $d\lambda_i$ should be set at 10-20% of the total reference load. At other load steps, $d\lambda_i$ can be defined by the analyst or automatically altered based on the degree of nonlinearity present within the structure at the given load step.

In the multimode procedure considered, the reference load is based on total seismic base shear. The applied base shear on the structure is determined by including the spectral

acceleration response spectra that corresponds to a performance objective of interest. FEMA 273 (1997) defines short and long period response spectra accelerations corresponding to 20%, 10%, and 2% probability of exceedance in a 50 year period. These accelerations are used to define the Immediate Occupancy, Life Safety, and Collapse Prevention hazard levels, respectively. To determine a total seismic base shear, the appropriate acceleration values are combined with the modal masses determined through the analysis (Grierson et al., 2006). The decision to pursue a force-based rather than displacement-based procedure was based on several factors. First, it has been shown that, when the acceleration response spectrum is based on site-specific ground conditions, force-based procedures are able to give good predictions of seismic demands (Gupta & Kunnath, 2000). Second, while displacement-controlled methods may be more rational for the rehabilitation of existing structures, force-based methods are more applicable to the design of new structures due to the fact that design earthquakes are represented by acceleration spectra which directly translates to a design governed by loads.

The method given by Grierson et al. (2006) is rooted in the method developed by Hasan et al. (2002) presented previously. Structural nonlinearity is accounted for via plasticity factors that are based on post-yield moment-curvature models. Thus, structural stiffness is accounted for during each load step based on the results of the previous load step and the rigidity of each member end connection is updated to reflect the stiffness degradation.

The process for including the effects of multiple modes is broken into two steps. First, multiple force-based single mode pushover analyses are performed for each mode of vibration to determine the corresponding modal response. Second, the responses of each individual mode are combined using an acceptable modal combination rule.

Executing the first half of the procedure requires eight sequential steps. The first is to determine the mode shapes, φ_k, under consideration. The mode shapes are determined using the same procedure outlined by the ATC-40 (1996) Capacity Spectrum Method. Grierson et al. (2006) computed the mode shapes for the first three modes of vibration, expressed within the procedure as n_m, the total number of modes to be considered, equal to 3. The first three modes were included because they were judged to have the most significant impact on the overall structural response. With modal shapes determined, the second step is to evaluate the effective modal mass of each mode by (Grierson et al., 2006):

$$M_k = \frac{(\varphi_k^T \boldsymbol{MI})^2}{\varphi_k^T \boldsymbol{M} \varphi_k} \qquad \text{Equation 2.3.4.1-3}$$

where **M** is the lump mass matrix and **I** is the unity vector. The modal masses are evaluated from *k* equal to one to *k* equal to n_m. Third, a lateral load profile vector is determined by (Grierson et al., 2006):

$$\boldsymbol{C}_k = \boldsymbol{M}\varphi_k \qquad \text{Equation 2.3.4.1-3}$$

The lateral load profile vector is assumed to be invariant over the entire loading history. Implicit in this assumption is that φ_k is invariant. The assumption of invariance is a notable one. As the structure yields and experiences stiffness degradation throughout the loading event, the vibrational properties of the structure also change which results in a redistribution of inertia forces. The result is a lateral load distribution that varies with time. In fact, for an inelastic system no invariant distribution of forces can effectively produce displacements proportional to the modal shape at all displacements or force levels (Chopra & Goel, 2002). Some effort has been made to develop adaptive force distributions that reflect the change in vibrational properties of the structure, however the computational effort associated with such procedures is very high and the conceptual basis highly complicated. The results given using adaptive force procedures may be of higher accuracy, but their difficulty of implementation makes them impractical and the associated increase in accuracy is not worth the increase in effort (Chopra & Goel, 2002). Being that the mission of Grierson et al. (2006) is to develop a computationally attractive multimode analysis procedure, the invariant force distribution is acceptable.

The fourth step is to compute the modal period, T_k, for the kth mode by (Grierson et al., 2006):

$$T_k = 2\pi \sqrt{\frac{\sum_{s=1}^{n_s}(m_s v_s^2)}{\sum_{s=1}^{n_s}(V_1 C_{k,s} v_s)}} \qquad \text{Equation 2.3.4.1-4}$$

where m_s is the seismic mass of story *s*, n_s is the number of stories, and $C_{k,s}$ are the entities of vector $\mathbf{C}_k$, V_1 is a base shear force taken to be sufficiently small to ensure that the resulting lateral displacement v_s of story level *s* corresponds to elastic behavior of the structure. The computation of the period of vibration for each mode under consideration is important to determine the level of seismic hazard that should be applied to the building. Going back to the parameters of the force-based pushover being used, a total design base shear is needed in order to set the point of termination for the pushover analysis. To compute a design base shear a spectral acceleration response is needed, and the spectral acceleration response, for each mode of vibration for each hazard level considered, can be determined only by calculating the

corresponding modal period. With the modal period known, the spectral acceleration value for each hazard level, i, for the kth mode, $S^i_{a,k}$ is determined by (Grierson et al., 2006):

$$S^i_{a,k} = \begin{cases} S^i_s\left(0.4 + \frac{3T_k}{T^i_0}\right) & 0 < T_k \leq 0.2T^i_0 \\ S^i_s & 0.2T^i_0 < T_k \leq T^i_0 \\ \frac{S^i_1}{T_k} & T_k > T^i_0 \end{cases} \quad \text{Equation 2.3.4.1-5}$$

where S^i_s is the short period response acceleration parameter for the given hazard level, S^i_1 is the one second period acceleration response parameter for the given hazard level, and T_0 is the period at which the constant acceleration and constant velocity regions of the response spectrum intersect for the design earthquake associated with hazard level i. The values used in the determination of the spectral acceleration value for each hazard level and mode are from FEMA 273 (1997) specifications. The value T_o is calculated based on tabulated values of damping coefficients and spectral response acceleration parameters modified based on site class. By utilizing site-specific ground motions, the total base shear, based on individual modal response, can be determined.

The total modal design base shear for each hazard level and mode, $V^i_{b,k}$, is given by the expression (Grierson et al., 2006):

$$V^i_{b,k} = M_k S^i_{a,k} \quad \text{Equation 2.3.4.1-6}$$

where all values have been previously defined. As can be seen, the total design base shear for each hazard level and mode depends upon the corresponding modal mass and corresponding spectral acceleration value. Once the base shear has been determined, a pushover analysis for each mode can be performed individually using the Euler method and terminating the analysis when the total design base shear is reached. Modal pushover curves for the first three modes of a sample structure are shown in Figure 2.3.4.1-1.

Figure 2.3.4.1-1 Sample Modal Pushover Curves

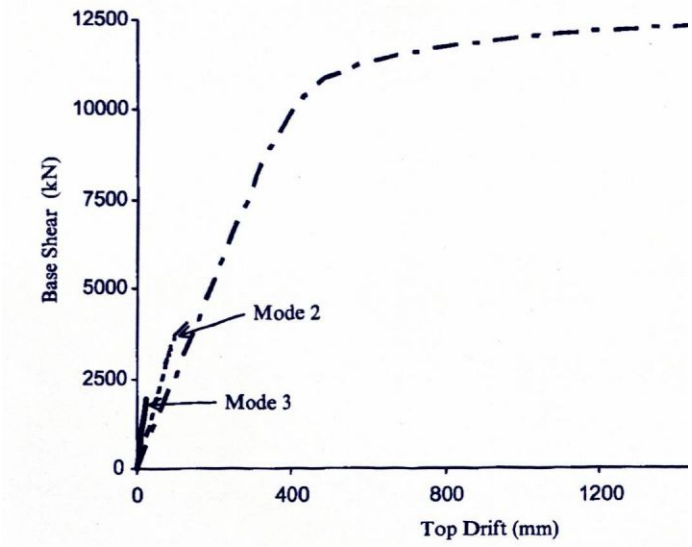

Source: Grierson, D., & Gong, Y., & Xu, L. (2006). Optimal performance-based seismic design using modal pushover analysis. *Journal of Earthquake Engineering, 10*, 73-96.

When the pushover analyses for each individual mode are complete and the appropriate response quantities extracted, the second step of this multimode procedure can be executed. The second step consists of combining each individual modal response into a total building response using the square-root-sum-of-squares (SSRS) method, which is written as (Grierson et al., 2006):

$$u_c = \sqrt{\sum_{k=1}^{n_m}(u_k^2)} \qquad \text{Equation 2.3.4.1-7}$$

where u_k is the structural response associated with the kth mode, u_c is the combined structural response, and n_m is the total number of modes considered. The structural response parameters by which the structure will be checked for performance are allowable roof drift ratio and allowable interstory drift ratios, both of which are specified in FEMA 273 (1997).

Using a nine-story steel frame structure, the multimode method described was compared against a single mode nonlinear static procedure. Grierson et al. (2006) found that the multimode method provides more accurate results than did the single mode method while retaining the computational attractiveness that would lead an analyst to select a multimode nonlinear static procedure over a nonlinear dynamic procedure. While several approximations were made in this procedure, including those already noted and the fact that the SRSS method is itself an approximate method, the multimode nonlinear static procedure described is a useful tool with justifiably accurate results given the simplicity of the procedure.

2.3.4.2 Modal Pushover Analysis

The second multimode nonlinear static procedure presented is rooted in classical structural dynamic theory. Developed by Chopra and Goel (2002), the modal pushover analysis (MPA) is based on a reformulation of the common response spectrum analysis and utilizes a modal expansion of effective earthquake forces. By expanding the anticipated effective earthquake forces into their modal components from a classical structural dynamics viewpoint, actual ground motion records (El Centro, in this case) can be used. Further, the new method is compared against the results of a rigorous nonlinear time history analysis and the results evaluated to determine the efficacy of the method.

In the procedures already discussed, we have seen several methods for determining a target displacement at which the pushover analysis is terminated. These methods have all been approximate in nature and have not been derived from actual analytical results but rather from various approximating factors. A new method for determining target displacement is now presented. The apex of analysis procedures, nonlinear time history analysis (discussed in the following section), is simplified into an uncoupled modal response history analysis (UMRHA) whereby the peak lateral roof displacement based on actual ground motion records for a nonlinear SDOF system is determined. This peak lateral displacement is used as the target displacement for the modal pushover analysis of an inelastic MDOF system.

The process begins by writing the effective earthquake forces applied on a system as (Chopra & Goel, 2002):

$$\boldsymbol{p}_{eff}(t) = -\boldsymbol{mi}\ddot{u}_g(t) \qquad \text{Equation 2.3.4.2-1}$$

where $\boldsymbol{i}$ is termed the influence vector and is equal to unity. To apply the effective earthquake force over the height of the building, the spatial distribution vector, $\boldsymbol{s}$, is defined as (Chopra & Goel, 2002):

$$\boldsymbol{s} = \boldsymbol{mi} \qquad \text{Equation 2.3.4.2-2}$$

In order to evaluate the structural response on a mode-by-mode basis, the spatial distribution can be expanded and written as a summation of the modal inertia force distribution, $\boldsymbol{s_n}$ (Chopra & Goel, 2002):

$$\boldsymbol{mi} = \sum_{n=1}^{N} \boldsymbol{s_n} = \sum_{n=1}^{N} \Gamma_n \boldsymbol{m\Phi_n} \qquad \text{Equation 2.3.4.2-3}$$

where $\boldsymbol{\Phi}_n$ is the nth natural vibration mode for the structure. The quantity Γ_n is defined by (Chopra & Goel, 2002):

$$\Gamma_n = \frac{L_n}{M_n} \quad \text{and} \quad L_n = \Phi_n^T \boldsymbol{mi} \quad \text{and} \quad M_n = \boldsymbol{\Phi}_n^T \boldsymbol{m} \boldsymbol{\Phi}_n \quad \text{Equation 2.3.4.2-4}$$

Using the definitions given, the effective earthquake forces can be expanded into their individual modal contributions and spatially distributed over the height of the structure by (Chopra & Goel, 2002):

$$\boldsymbol{p}_{eff}(t) = \sum_{n=1}^{N} \boldsymbol{p}_{eff,n}(t) = \sum_{n=1}^{N} -\boldsymbol{s}_n \ddot{u}_g\,(t) \qquad \text{Equation 2.3.4.2-5}$$

where the individual contributions of each mode to the spatial distribution vector is given as (Chopra & Goel, 2002):

$$\boldsymbol{s}_n = \Gamma_n \boldsymbol{m} \boldsymbol{\Phi}_n \qquad \text{Equation 2.3.4.2-6}$$

By writing the inertia force distribution in terms of individual modes, we can also say that the response of the system to the effective modal earthquake force is due only to the nth-mode. To simplify the process of attaining a peak lateral displacement we introduce a value, $D_n(t)$, which is a modal response co-ordinate governed by the equation of motion for a linear SDOF system with the same angular natural frequency and natural damping ratio as the MDOF system. The floor displacements of the MDOF system can then be written as (Chopra & Goel, 2002):

$$\boldsymbol{u}_n(t) = \Gamma_n \boldsymbol{\Phi}_n D_n(t) \qquad \text{Equation 2.3.4.2-7}$$

By applying the modal spatial distribution of forces due to the effective earthquake force on the building statically, we can determine any modal static response, $r^{st}{}_n$. And by defining the pseudo acceleration response of the nth-mode for the SDOF system, $A_n(t)$, as the SDOF modal coordinate, $D_n(t)$, times the angular natural frequency squared, any dynamic response quantity can be calculated by (Chopra & Goel, 2002):

$$r_n(t) = r_n^{st} A_n(t) \qquad \text{Equation 2.3.4.2-8}$$

The equations so far given will form the basis of the manipulations required to construct an UMRHA procedure (Chopra & Goel, 2002). Also, the equations given describe an elastic system and must be adjusted to reflect an inelastic system. Finally, the equation of motion for the elastic SDOF system is given by (Chopra & Goel, 2002):

$$\ddot{D}_n + 2\zeta_n \omega_n \dot{D}_n + \omega_n^2 D_n = -\ddot{u}_g(t) \quad \text{Equation 2.3.4.2-9}$$

These equations will form the foundation of the method as we move on to develop the inelastic equation of motion for use in the UMRHA procedure (Chopra & Goel, 2002).

If we were presently interested in developing a procedure for a nonlinear time history analysis, development of the inelastic equation of motion would show that the lateral forces at *N* floor levels depends on the history of the displacement (Chopra & Goel, 2002):

$$\boldsymbol{f}_s = \boldsymbol{f}_s(\boldsymbol{u}, sign\ \dot{\boldsymbol{u}}) \quad \text{Equation 2.3.4.2-10}$$

And, for the nonlinear time history form, the resisting force is equal to (Chopra & Goel, 2002):

$$F_{sn} = \boldsymbol{\Phi}_n^T \boldsymbol{f}_s(\boldsymbol{u}, sign\ \dot{\boldsymbol{u}}) \qquad \text{Equation 2.3.4.2-12}$$

In doing so, it becomes evident that the resisting force of the nth-mode is dependent on all modal coordinates (Chopra & Goel 2002). The vector character of the displacement quantities, *u*, bears this point out. The modal coordinates are coupled due to the nonlinear behavior of the structure. In the aim of developing a computationally attractive multimode procedure, this creates a problem. Solving the coupled equations is computationally burdensome and cannot be done conveniently by standard software. The coupling of the modal coordinates whereby each individual modal resisting force is dependent on all modal coordinates is the barrier that must be overcome.

The approximate UMRHA procedure is arrived at by neglecting the coupling of the modal coordinates. This assumption is deemed acceptable because although modes other than the nth-mode will participate in the solution, the nth-mode solution will be dominant. Chopra and Goel (2002) illustrate this point by performing a nonlinear time history analysis on the first three modes of the structure. Numerical results show that the contributions of the second and third mode responses to the first mode response are only small fractions of the first mode response. Similarly, contributions by the first and third mode response on the second mode response are insignificant. Thus, the assumption is deemed valid.

Finally, with the modal coordinates uncoupled, the nonlinear equation of motion becomes (Chopra & Goel, 2002):

$$\ddot{D}_n + 2\zeta_n \omega_n \dot{D}_n + \frac{F_{sn}}{L_n} = -\ddot{u}_g(t) \qquad \text{Equation 2.3.4.2-13}$$

And the modal resisting force, in its uncoupled form, can be written as (Chopra & Goel, 2002):

$$F_{sn} = \boldsymbol{\Phi}_n^T \boldsymbol{f}_s(D_n, sign\ \dot{D}_n) \quad \text{Equation 2.3.4.2-14}$$

where the resisting force of the nth-mode now depends only on one modal coordinate. This simplification is important when viewed in terms of the stated goal for the development of this procedure. Because the modal coordinates are now uncoupled, the equation of motion can now be solved conveniently by commercial software because it is of the same form as the standard

equation for an SDOF system. Now, the equations for determining floor displacement, $\boldsymbol{u}$, and any response quantity, r_n, can be used in conjunction with the nonlinear equation of motion to give dynamic analysis results for the nonlinear SDOF system (Chopra & Goel, 2002).

The approximate UMRHA method is a powerful component for use in a multimode nonlinear static analysis for two reasons. First, the manipulations made during the derivation of the UMRHA procedure form the basis of the modal pushover analysis to be presented next. Second, the UMRHA serves as an efficient tool to compute, with acceptable accuracy, the anticipated peak roof displacement from a dynamic analysis based on actual ground motion records. In this way, the UMRHA is a very useful augmentation to the multimode nonlinear static procedure as it computes a target lateral displacement that is less approximate than the methods discussed earlier.

Finally, the modal pushover analysis can be developed (it should be noted that modal pushover and multimode nonlinear static analysis are used analogously). First, the peak nth-mode response, r_{no}, can be determined from (Chopra & Goel, 2002):

$$r_{no} = r_n^{st} A_n \quad \text{Equation 2.3.4.2-15}$$

Additionally, by distributing modal contributions of the effective earthquake force over the height of the building and performing static analysis using (Chopra & Goel, 2002):

$$\boldsymbol{s}_n^* = \boldsymbol{m}\Phi_n \quad \text{Equation 2.3.4.2-16}$$

the peak nth-mode response value can also be determined. By evaluating the nonlinear equation of motion for D_n using UMRHA, the target peak lateral displacement at the roof is given by (Chopra & Goel, 2002):

$$u_{rno} = \Gamma_n \Phi_{rn} D_n \quad \text{Equation 2.3.4.2-17}$$

and the pseudo acceleration can readily be determined from D_n as described above. When the peak modal responses, r_{no}, have been determined for each mode of interest, the total peak value of the response, r_o, can be found by combining the individual modal responses using the SSRS modal combination rule (Chopra & Goel 2002). Again, at the target roof displacement, any response quantity for the MDOF inelastic system can be determined.

Comparing the results of the modal pushover analysis to the results of a rigorous nonlinear time history analysis for an example structure illustrates that the accuracy of the modal pushover analysis varies on the response quantity of interest. The modal pushover analysis yields good results for story drifts, roof displacements, and detected the formation of most plastic

hinges. However, plastic hinge rotations were not determined with as much accuracy. Chopra and Goel (2002) conclude that the modal pushover analysis procedure developed is accurate enough for most practical implementations.

Nonlinear static procedures can take many unique forms. Those methods presented herein do not represent the entire spectrum of nonlinear static procedures, but do offer a good cross section of the methodologies available. Single mode procedures are limited in their application to low to mid-rise buildings with natural period of vibration of about one second or less. Multimode procedures seek to extend the use of nonlinear static procedures into taller structures with longer periods. While both single and multimode procedures have been shown to produce generally good results, the situations in which their results are not suitable are many and ill-defined. Nonlinear static procedures are simplified procedures and as such are fundamentally limited in their applicability to certain structures. However, the number of structures that can be sufficiently analyzed using nonlinear static procedures is continually growing with the pace of ongoing research. For structures where nonlinear static procedures are verifiably and certainly applicable, the nonlinear static procedures are attractive in that they achieve very good results with a computational burden that is significantly less than for nonlinear dynamic procedures.

2.4 Nonlinear Dynamic

The final category of analysis procedures given by FEMA, nonlinear dynamic procedures, is the most computationally difficult and the most accurate. Nonlinear dynamic procedures have no restrictions as far as their applicability to various types of structures, though they are the only option for highly irregular structures or for structures that may have especially long natural periods of vibration. By applying actual ground motion records (accelerograms) to models that explicitly consider both geometric and material nonlinearity nonlinear dynamic procedures eliminate uncertainty of results to the greatest degree compared to other analysis procedures. Obviously, the analytical models required to execute a trustworthy nonlinear dynamic analysis are extremely complex as they must directly consider a number of inelastic behavior parameters including positive and negative yield moments, Euler elastic and inelastic buckling loads, and type of yield surface (Alimoradi, Pezeshk, & Foley, 2004). However, this increase in computational burden is rewarded. Nonlinear dynamic analysis is able to give more

accurate response quantities for the simple fact that it directly captures all modes of vibration, all forms of nonlinearity, and second order effects (Foley, Pezeshk, & Alimoradi, 2007).

To date, nonlinear dynamic analysis has not been widely applied in design practice. The reasons for this are several: understanding system response is highly difficult as a large amount of data is produced and its interpretation requires extensive experience, reliable ground motion input records must be available, and current design procedures involve a large amount of trial and error (Foley et al., 2007). However, nonlinear dynamic procedures are currently gaining momentum as: research has resulted in the development of practical model codes, future probabilistic PBSD procedures are being planned and discussed, and computing power has helped to automate the time intensive trial and error procedure (Foley et al., 2007). These developments have raised the profile of nonlinear dynamic analysis as a practically available analysis tool and fostered further research into its use.

The efficacy of nonlinear dynamic procedures is highly susceptible to the quantity and types of input ground motion records used. Indeed, the reliability of results of such procedures "depend on the use of realistic ground motion records with phasing and response spectral characteristics that are appropriate for the magnitude, distance, site conditions, and wave propagation properties of the region" (Farrow & Kurama, 2003). To address this issue, FEMA 356 (2000) has specified the type and quantity of ground motion records that must be used to complete a reliable time-history analysis. First, a time-history analysis must be performed with at least three data sets of ground motion that have magnitude, fault distances, and source mechanisms consistent with those that control the design earthquake ground motion. Further, for each ground motion data set the SRSS of the 5%-damped site-specific spectrum of the scaled horizontal components must be constructed. The scaling of the data sets must ensure that the average value of the SRSS spectra constructed is not less than 1.4 times the 5%-damped spectrum for the design earthquake for periods between 20% of the building's fundamental period and 150% of the building's fundamental period. When three data sets are used, the maximum value of each response parameter must be used to evaluate the design. For cases where seven data sets or more are used, the average value of each response parameter may be used for evaluation (FEMA 356, 2000).

As mentioned, nonlinear time-history analysis requires the consideration and implementation of a huge number of parameters and sub-models (hysteresis, yielding, etc.). For

our purposes, we briefly examine the governing equation of motion for a nonlinear system (Chopra, 2007):

$$\boldsymbol{m\ddot{u}} + \boldsymbol{c\dot{u}} + \boldsymbol{f}_s(\boldsymbol{u}, \dot{\boldsymbol{u}}) = -\boldsymbol{m\iota}\ddot{u}_g(t) \quad \text{Equation 2.4-1}$$

where all terms have been previously defined. This equation must be evaluated at each (very short) time step and the structural stiffness matrix must be reformulated at every time instant from the element tangent stiffness matrices that account for the behavior of each element at that time step. The time steps must be kept short enough that the numerical procedure is accurate, converges to a solution, and remains stable. The behavior of each element must be considered, whether the element is on the initial loading, unloading, or reloading of the defined element force-deformation relationship. While the UMRHA procedure was introduced previously, the coupled resisting force and displacement elements in a nonlinear time-history analysis may not be uncoupled, resulting in the complex problem of solving the coupled differential equations simultaneously. The numerical solution can be computed by a variety of methods (Chopra, 2007).

In addition to being highly sensitive to the quantity and type of ground motion records used, nonlinear time-history analyses are also highly sensitive to the type of model used and the assumptions made, especially when considering P-Δ effects. Thus, the selection of whether and how to include parameters like panel zone size, panel zone strength and stiffness, interior gravity columns, floor slabs, shear connections, and others may have a profound effect on model output (Chopra, 2007). Additionally, the record to record variability inherent in input records requires statistical manipulation of results to truly determine a representative structural response. Because of these observations, it is clear that nonlinear time-history analyses should only be executed by the most experienced engineering design professionals.

A useful enhancement to nonlinear time-history analysis, Incremental Dynamic Analysis, is a procedure for generating useful graphical tools used in evaluating the complete range of structural response.

2.4.1 Incremental Dynamic Analysis

The nonlinear time history analysis procedure previously discussed uses a suite of ground motion records and produces a suite of single-point analyses which are primarily used for checking the designed structure. In the case of pushover analysis, however, the pushover curve

provides a continuous view of the total structural behavior and can describe elastic, yielding, post-yielding, and collapse behavior. The reasoning behind incremental dynamic analysis (IDA) is similar to the reasoning behind pushover analysis. The observation that static pushover curves greatly increase our understanding of a structure's behavior has led to the development of a similarly continuous picture of structural behavior for dynamic systems: incremental dynamic analysis. The objectives of IDA are: complete understanding of the range of response against the range of possible levels of ground motion, improved understanding of the effects on structures of more severe ground motion levels, improved understanding of the alterations in the nature of the structural response with increasing ground motion intensity, and producing estimates of the dynamic capacity of a global structural system (Vamvatsikos & Cornell, 2002).

The goal of IDA is development of the IDA curve. The general process for developing the curve consists of six essential steps: determine an appropriate intensity measure (IM), determine an appropriate damage measure (DM), define an appropriate scaling of the ground motion record(s), perform a nonlinear time-history analysis for each scaled ground motion input, plot the results of IM versus DM from the analysis output, and use interpolation to smooth the curve. By following this procedure, a smooth curve of the total structural response, from the elastic range to global instability, can be determined for a given ground motion record. Repeating this process for the same structure for multiple ground motion inputs yields an IDA curve set that can be statistically manipulated to give probabilistic mean annual frequencies of exceedance for use within the PBSD framework.

An intensity measure, or monotonic scalable ground motion intensity measure, is a non-negative scalar that describes the intensity of a ground motion record that increases monotonically with the scale factor. A scale factor, λ, is a non-negative scalar that is multiplicatively applied to a natural acceleration time history, the result of which is a scaled accelerogram. An IM could be any parameter that effectively describes the intensity of the scaled ground motion for a given structure. Typical IMs include peak ground acceleration, peak ground velocity, and the 5%-damped spectral acceleration at the structure's first mode period. Additionally, IMs are proportional to the scale factor (Vamvatsikos & Cornell, 2002).

Definition of an appropriate IM forms the demand input for the structure to be evaluated, and so we now need a parameter by which we can monitor the response of the structure. Such a parameter is termed the damage measure (DM). A DM may be any observable quantity that is

either explicitly provided by a nonlinear dynamic analysis or that may be deduced from the analysis results. The most often used damage parameter is peak interstory drift ratio. There are two reasons for peak interstory drift ratio being a common DM selection: first, structural performance levels, as defined by FEMA, are generally quantified by peak interstory drift ratio limits, and second, peak interstory drift ratio is well connected to other important response quantities: joint rotations and global and local story collapse. It may often be pertinent to select multiple DMs to measure several different response characteristics and create a wider picture of limit states and failure modes. If multiple DMs are used, they are all subjected to the same IMs (Vamvatsikos & Cornell, 2002).

The concept of charting an IDA curve is simple enough: for each individual scaling step plot the appropriate IM against the DM captured through nonlinear time-history analysis as a single point and continue this procedure until the curve has been sufficiently defined. In practice, however, efficiently developing a sufficiently descriptive IDA curve is a difficult procedure. The main difficulty lies in prescribing enough steps in the scaling process to draw the curve with proper resolution (i.e., capturing the full curve behavior) from elasticity to collapse without imposing an unnecessarily heavy computational burden with gratuitous steps. Moreover, the process of scaling a record, running a nonlinear time-history analysis, extracting the appropriate DM value, rescaling a record, running another nonlinear time-history analysis, etc. is a time consuming one. The solution to both problems would be the implementation of an effective algorithm that could autonomously select appropriate scaling factors and proceed through an entire curve development process without constant analyst supervision. The hunt and fill algorithm (Vamvatsikos & Cornell, 2002) is that effective algorithm.

The hunt and fill algorithm is actually the result of the sequential run of three individual algorithms. The algorithm's task is to simultaneously achieve a high demand resolution and a high capacity resolution (Vamvatsikos & Cornell, 2002). Demand resolution refers to a scaling of the IM by which the points on the curve are spread evenly such that the gap in IM values between points is smaller than some defined tolerance. Capacity resolution requires a concentration of points, in terms of scaled IM values, around important events in the life of the IDA curve. The most critical event of an IDA curve is the location at which the curve moves into a flatline behavior. A flatlining of the IDA curve denotes dynamic instability and subsequently collapse. By defining a dense concentration of IM values (and corresponding DM

values) in the region of flatline behavior, we can effectively bracket the response and capture the subtleties in behavior that an informative IDA curve requires. We can state the capacity resolution requirement by saying that we desire the distance between the highest non-collapsing run and the lowest collapsing run to have IM values less than some defined tolerance. Collapsing runs are those that fail to numerically converge or that violate some predefined collapse rule. Finally, we expect the hunt and fill algorithm to execute these tasks in as few runs as possible to minimize the overall computational time (Vamvatsikos & Cornell, 2002).

The first of the three individual algorithms that comprise the hunt and fill algorithm is a stepping algorithm. For this case, the IM is increased by a constant increment from zero to structural collapse. The stepping algorithm will generate an IDA curve with a uniform distribution of IM points from which each corresponding DM is extracted. The process needs only two definitions: the stepping increment and a point of termination (a collapsing run). By making the required definitions, the algorithm acts to repeatedly increase IM values by the defined step, scale the accelerogram record, run the analysis and extract the DM until the defined collapse state is reached. The upside to this routine is that it is easy to program. The downside is that the quality of the resulting curve is heavily dependent on the defined IM increment step and so is probably not cost-efficient (Vamvatsikos & Cornell, 2002).

The second routine is a hunting algorithm. An appreciable development would be if we could find a way to speed convergence towards the curve's flatline behavior. This can be done by increasing the IM steps by a factor, thus generating a geometric series of IM values. In this way, the flatline behavior can be effectively bracketed without dramatically increasing the number of runs and saving computational time. The hunting algorithm functions by repeating the following steps: increase the IM value by the step quantity, scale record, run analysis, extract DM values, and increase the step. This process continues until collapse is reached (Vamvatsikos & Cornell, 2002).

Finally, a procedure must be implemented that can reduce the number of steps, tighten the bracketing of the flatline, and allow a defined accuracy for the capacity to be reached independently of the demand resolution. This process improves the capacity resolution by executing these steps when numerical non-convergence (collapse) is first detected. To do this, the following steps are repeated: select an IM in the space between the highest non-collapsing and lowest non-collapsing IM values, scale the accelerogram record, run the analysis, and extract

the DM values. This process terminates when the gap in IM values between the highest collapsing and lowest non-collapsing runs are less than a defined tolerance (Vamvatsikos & Cornell, 2002). By executing the hunt and fill algorithm, consisting of the three separate portions discussed run sequentially, an efficient parameter for generating and plotting a large amount of data is arrived at. The hunt and fill algorithm bounds the IM parameter space, fills in demand and capacity gaps, and uses increasingly large steps to achieve those ends.

The result of the complete execution of the hunt and fill algorithm is a string of discrete points, each with an IM value and corresponding DM value, that forms the outline of the IDA curve. The next step is to appropriately smooth the curve by connecting the individual points to create a continuous response backbone. In doing so, the curve becomes even more useful, as any arbitrarily selected IM value will give the resulting DM value for the structure. Smoothing the curve is done by interpolation of the existing points determined from nonlinear time-history analysis and the hunt and fill algorithm. Vamvatsikos and Cornell (2004) use a superior spline interpolation. The interpolation is able to realistically interpret the existing points into a smooth curve that is an accurate representation of what we would expect if we had executed enough runs to define the curve continuously using individual discrete points. Clearly, the computational effort in doing so would have been tremendous. Interpolating the few existing points allows the analyst to extract continuous information from the curve with a minimum number of analyses.

The discussion of IDA curves so far has examined the process by which a single IDA curve, for a single ground motion record, can be determined. Given the FEMA requirements concerning ground motion records, it is clear that a single IDA curve is insufficient to confidently portray the response of a structure. Therefore, we must be able to develop an IDA curve set, an example of which is shown in Figure 2.4.1-1, which is a collection of IDA curves for the same structure for the same IMs and DMs each subjected to a different ground motion record.

Figure 2.4.1-1 Sample IDA Curve Set

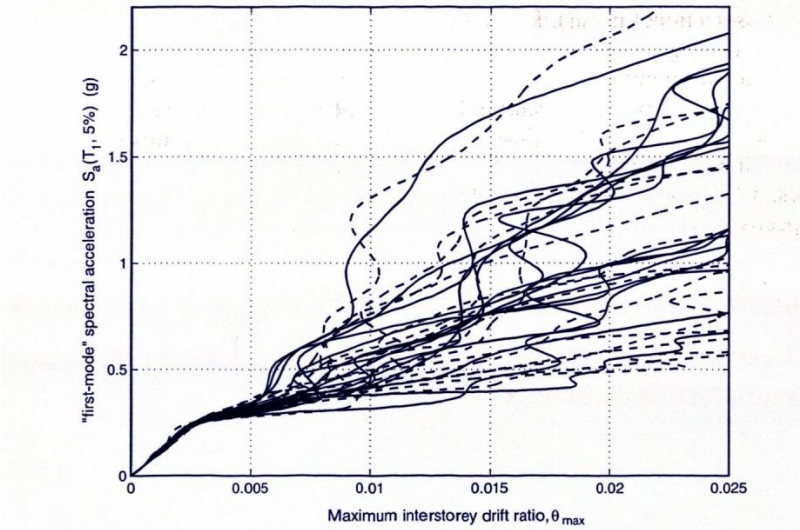

Source: Vamvatsikos, D., & Cornell, C. (2002). Incremental dynamic analysis. *Earthquake Engineering and Structural Dynamics, 31*, 491-514.

Each individual curve in a curve set is developed and plotted in the same fashion as described above. After each individual curve has been established, they must be summarized. The multiple individual deterministic curves must be combined into unified probabilistic expressions of structural response given the ground motion input. This is done by using spline interpolation with cross-sectional fractiles (Vamvatsikos & Cornell, 2004). The spline interpolation (used previously to smooth the individual IDA curves) can generate stripes of DM values for arbitrary values of IM where each stripe contains a quantity of DM values equal to the quantity of ground motion records used. The DM values for each stripe can be summarized into 16%, 50%, and 84% percentiles and subsequently we arrive at fractile values of DM given IM. The fractile values are then interpolated again to create the 16%, 50%, and 84% fractile IDA curves, examples of which are shown in Figure 2.4.1-2 (Vamvatsikos & Cornell, 2004).

Figure 2.4.1-2 Sample IDA Fractile Curves

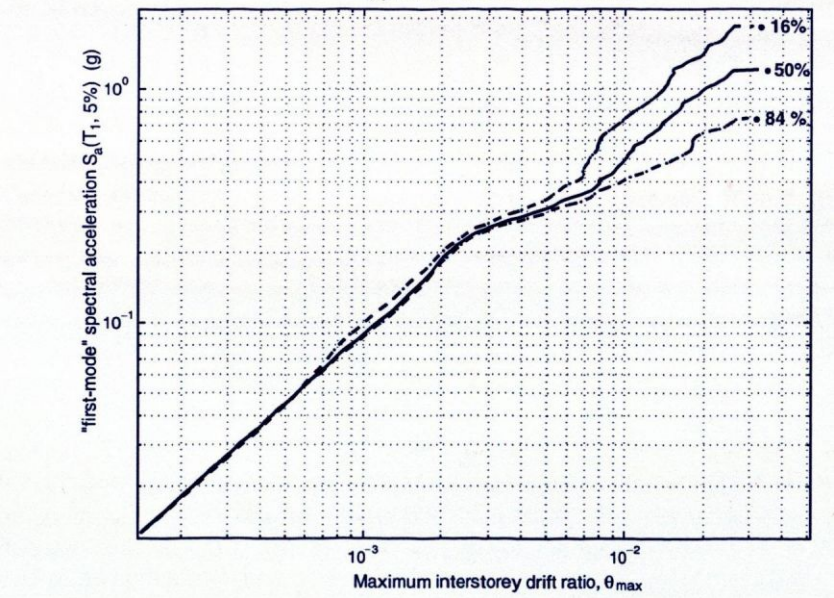

Source: Vamvatsikos, D., & Cornell, C. (2002). Incremental dynamic analysis. *Earthquake Engineering and Structural Dynamics, 31*, 491-514.

Thus, each IDA fractile curve shows the percentage of ground motion records that elicit from the structure a DM value at a given IM value. The curves provide a statistical decision-making tool. The 16% IDA fractile curve, for example, can be interpreted as the DM value experienced by the structure for 16% of the ground motion records for a given IM.

The next important consideration for the IDA procedure is how to incorporate it into a PBSD framework. This question really comes down to how limit states can be defined on the curve.

Limit states can be defined by either a DM-based or IM-based rule, with the former being the simpler of the two. Each rule is illustrated in Figure 2.4.1-3 and 2.4.1-4, respectively. Based

Figure 2.4.1-3 Sample DM-Based Limit State Rule

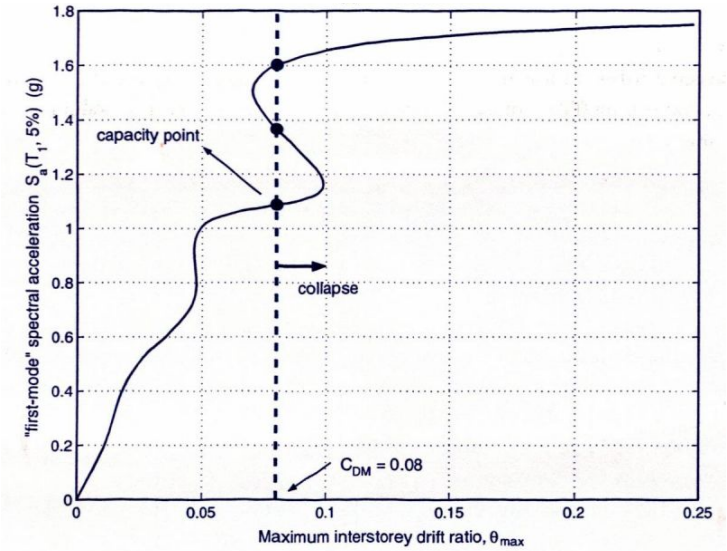

Source: Vamvatsikos, D., & Cornell, C. (2002). Incremental dynamic analysis. *Earthquake Engineering and Structural Dynamics, 31*, 491-514.

Figure 2.4.1-4 Sample IM-Based Limit State Rule

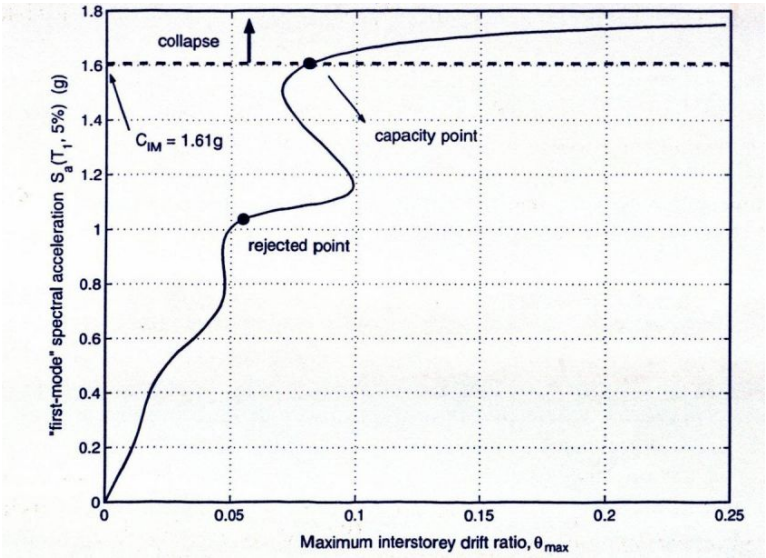

Source: Vamvatsikos, D., & Cornell, C. (2002). Incremental dynamic analysis. *Earthquake Engineering and Structural Dynamics, 31*, 491-514.

on FEMA structural performance level limit quantities, a vertical line can be drawn on the IDA curve beyond which the structure is said to violate the limit state. In this way, Immediate Occupancy and Operational performance levels can be quickly illustrated on the curve by drawing a vertical line at the appropriate DM value. In the case where a limit state line crosses the IDA curve at multiple locations, the governing case can be chosen based on the coordinate for which the IM value is the lowest. IM-based rules are used to assess a structure's collapse

capacity: the collapse prevention performance level. A horizontal line is drawn on the IDA curve at a constant IM level above which the structure is considered collapsing and below which the structure is non-collapsing (Vamvatsikos & Cornell, 2002). The IM level for which the defining collapse prevention line is drawn occurs when either the straight line tangent slope between two consecutive points is less than 20% of the initial elastic slope or the peak interstory drift ratio exceeds 10%, whichever occurs first in terms of IM values (FEMA 350, 2000). Implementing these performance level definitions into the IDA curve yields an even more effective tool. At the location of intersection between the limit state line and the IDA curve the performance of the structure can be immediately evaluated based on the hazard conditions and the structural performance either accepted or rejected based on the originally defined performance objective. In this way, we see that IDA curves are highly useful graphical and analytical tools that fit well into the framework of PBSD.

The IDA procedure has also found a place within the FEMA 350 (2000) guidelines. Unlike the method proposed by Vamvatsikos and Cornell (2002 & 2004), the FEMA 350 method does not suggest curve interpolation and suggests that only the median of the IDA curve set need be calculated rather than the various fractile curves presented above. Further, FEMA 350 (2000) utilizes incremental dynamic analysis only for the evaluation of global stability capacity. While IDA is certainly particularly well suited to evaluating the collapse of the structure, the steps provided above whereby other performance levels can be evaluated are important additions.

We now turn our attention to how IDA can be practically implemented to solve design problems within a PBSD context. The example considered, while not as rigorous in method as that proposed by Vamvatsikos and Cornell (2002 & 2004), nonetheless provides useful insight. The nature of PBSD leads design problems towards what can be termed a system identification problem. By selecting performance objectives for a building with known geometry, the only gap to be filled is the design of the LFRS. Performance objectives define both the seismic hazard and the desired structural damage limit states and so it is the engineer's task to design a system that, subjected to the given seismic hazard, will probabilistically achieve the performance desired. IDA curves are well suited to helping the designer fill in these gaps.

The process begins by developing a "target" IDA curve (van de Lindt, Pei, & Liu, 2008). This curve is constructed by plotting points corresponding to the desired performance objective: a drift limit and its associated first period 5%-damped spectral acceleration constitutes a single

point and represents a single performance objective. For this example, three such points are plotted, each representing a discrete performance level. Straight lines connect the individual points and represent the target IDA curve. The development of such a curve allows the engineer to determine an optimum design (in regard to the proportioning of the LFRS given the hazard and drift limit) at numerous seismic intensities. The example utilizes the 16% fractile IDA curve concept introduced above and essentially uses it as a measure of exceedance probability; which is to say that should the design adhere to the 16% fractile target IDA curve, the resulting design will have an 84% probability of not having its capacity exceeded.

The system identification procedure is a process where IDA is used to back out specified model parameters that will, ideally, lead the model to conform to the predefined target IDA curve (van de Lindt et al., 2008). Model parameters, in this case, refer to parameters that define the hysteresis model used in the global structure model. The hysteresis model used has ten parameters that define it, but by utilizing a response data base of tested structural assemblies (wood shear walls, in this case) it was found that nine parameters can be determined by empirical relationships from a single parameter: initial stiffness, K_0 (van de Lindt et al., 2008). The procedure, then, is to begin by selecting a single point on the target IDA curve. Next, a single earthquake record (of a suite of 20) is scaled to the IM defined by the point on the target curve. Last, a nonlinear time-history analysis is executed that will determine the initial stiffness that satisfies the target DM given the target IM (van de Lindt et al., 2008).

The model parameter determined by the analysis is not calculated on a deterministic basis. Rather, the initial stiffness, K_0, or other parameter of interest is calculated based on a random variable, X_p, from the conditional probability equation (van de Lindt et al., 2008):

$$P_t - \chi(F_{Xp}(x|S,E)) = 0 \qquad \text{Equation 2.4.1-1}$$

where P_t is the target probability value, F_{Xp} is the conditional cumulative distribution function (CDF), E is the seismic loading (ground motion records), χ is the general operator on the performance distribution that will yield the target probability, and S are the parameters of the nonlinear model. By defining a target probability of exceedance, say 16%, one can calculate an S (where K_0 is of particular interest) that satisfies the conditional probability equation given with a corresponding CDF. By executing the system identification procedure for each point on the target IDA curve for all ground motion records considered, a statistical distribution of the model parameter of interest can be generated.

From a chart of K_0 versus CDF, discrete points can be chosen that satisfy the probability of exceedance desired. This chart forms a curve of all possible system designs that satisfy the DM given IM requirements of the target IDA curve in terms of their respective exceedance probabilities. In this way, the IDA process can be a probabilistic design tool that is well suited to evaluating a structure's ability to meet a predefined PBSD performance objective. By selecting a point on the CDF versus K_0 graph, the initial stiffness value conforming to the desired IM, DM, and probability of exceedance can be determined and from that initial stiffness the other nine parameters for the system can be deduced. With these properties in hand, the engineer can design the system. Finally, with all system properties defined, a full incremental dynamic analysis procedure can be run and compared to the target IDA curve. The actual IDA curve developed is deemed acceptable if it at least exceeds (in terms of IM) the target IDA curve.

2.5 Assessing Confidence

No matter the analysis procedure used, the important final step of any performance objective evaluation procedure is the computation of a level of confidence associated with the probability that a structure will have less than a specified probability of exceedance of a desired performance level. One can never be absolutely certain that the level of seismic hazard used to evaluate performance is absolutely the level of seismic hazard the structure will experience during its life. Therefore, probability of exceedance, or mean annual frequency (MAF) of exceedance, is critical for determining the likelihood that the performance objective the analysis has verified will actually be met and our confidence in that likelihood. Multiple routes to this end exist, though most begin by computing a confidence parameter, λ (FEMA 350, 2000):

$$\lambda = \frac{\gamma \gamma_a D}{\varphi C} \qquad \text{Equation 2.5-1}$$

where C is a median estimate of capacity, D is calculated demand, γ is the demand variability factor, γ_a is the analysis uncertainty factor, and φ is a resistance factor that accounts for uncertainty. The confidence parameter should be computed for each response quantity used to evaluate performance and lower values of λ correspond to higher levels of confidence. FEMA 350 (2000) terms this consideration demand and resistance factor design (DRFD). The demand variability factor accounts for the uncertainty in actual earthquake ground motion and varies based on performance objective selected and height of the structure. The analysis uncertainty factor accounts for the bias and uncertainty of the analytical procedure used. The value

computed for λ by the above equation can be used in the next equation to extract a confidence level, q, from a set of tabulated values developed by FEMA 350 (2000). The following equation is back-calculated for K_X from which a confidence level, q, can be determined (FEMA 350, 2000):

$$\lambda = e^{-b\beta_{UT}(K_x - \frac{k\beta_{UT}}{2})} \quad \text{Equation 2.5-2}$$

where b is a coefficient relating the incremental change in demand to an incremental change in ground shaking intensity at the hazard level of interest, β_{UT} is an uncertainty measure equal to the vector sum of the logarithmic standard deviation of the variations in demand and capacity resulting from uncertainty, k is the slope of the hazard curve in ln-ln coordinates at the hazard level of interest, and K_X is the standard Gaussian variate associated with probability x of not being exceeded as a function of the number of standard deviations above or below the mean found in standard probability tables. Procedures for computing the unknown individual quantities are given in FEMA 350 (2000). The previous equation can be evaluated by the designer for each individual circumstance such that a set of unique confidence level values, q, can be determined. However, the effort associated with such a task is considerable and generally the effort expended will not be rewarded with a proportional improvement in confidence. Therefore, making good use of the values tabulated in FEMA 350 (2000) is the most efficient route for establishing a confidence level.

The other way to satisfy the probabilistic demands of PBSD is to compute an MAF of exceedance. A mean annual frequency of exceedance is a quantity from which a return period can be computed where the return period is equal to the inverse of the MAF. FEMA documents state hazard levels corresponding to performance objectives in terms of return period: 72 years for Immediate Occupancy, 475 years for Life Safety, and 2475 years for Collapse Prevention (FEMA 273, 1997). These return periods are based on the 50 year probabilities of exceedance given previously. This procedure is particularly useful when ground motion records are involved. The response of a structure due to a suite of ground motion records can be expressed as the MAF of exceeding a pre-defined performance parameter given the seismic hazard. "Using the geometry and location with respect to the site of all possible seismic sources, the probability distribution of earthquake magnitudes at each source and attenuation relationships, a conventional probabilistic seismic hazard analysis permits the estimations of the MAF of exceedance of a certain peak ground motion parameter by integration over all possible sources,

earthquake magnitudes and distances" (Ruiz-Garcia & Miranda, 2007). Such an integration may take the form of (Fragiadakis & Papadrakakis, 2008):

$$\lambda(EDP > edp) = \int_0^{\infty} [1 - P(EDP > edp/IM = im)] \left|\frac{d\lambda(IM)}{dIM}\right| dI \quad \text{Equation 2.5-3}$$

where λ is the MAF of a limit state, *EDP* is the structure's capacity for a given engineering demand parameter, *edp* is the demand due to ground shaking of the same engineering demand parameter, the term *P(EDP>edp/IM=im)* is the limit-state probability that *EDP* exceeds a threshold value conditional on the given intensity value *im*, and the second term in the above equation is the mean annual rate of ground motion intensity, *IM*, or the slope of the hazard curve. The hazard curve is "the MAF of exceedance computed for a wide range of pseudo-acceleration spectral ordinates" which is the primary result of a conventional probabilistic seismic hazard analysis (Ruiz-Garcia & Miranda, 2007). The integral can be evaluated by combining information taken from the structural analysis and information produced by seismologists. By taking the inverse of the resulting λ value, the earthquake return period in years can be calculated and then compared to the specified return periods given by FEMA 273 to check for compliance with the performance objectives. The execution of the foregoing procedure is a useful method for taking into account the record to record variability of a suite of ground motions and arriving at a probabilistic solution.

CHAPTER 3 - Optimization

Though the documents that have defined the framework for PBSD have not mentioned it directly, structural optimization is clearly a logical extension of the stated goals of PBSD: minimize cost while minimizing risk. A structural optimization scheme is, at its most basic, a process where the goal is to achieve a workable structural system at a minimum of expense. Optimization schemes become more specialized, and often more complex, depending on how one defines "expense" and what constitutes a "workable structural system" in each particular situation. Typically, these definitions tend to be expansive and result in a scheme that seeks to achieve an optimum solution given several objectives. Many or all of these several objectives may be in direct competition with another, i.e., it is not possible to minimize/maximize them simultaneously. Such a situation is termed a multi-objective optimization procedure, and defines the type of problem almost always at hand when working within a PBSD framework. The aim of this section is to establish a foundation of understanding and frame of possibility when working with PBSD structural optimization problems. Subsequent sections will consider the basis for structural optimization, examine the algorithms necessary to implement an optimization procedure, determine the fundamental parts of any optimization procedure, and finally consider unique aspects to optimization for different system materials.

3.1 Priorities & Purpose

It is not possible to purchase the best possible product at the absolute lowest possible cost. In all products, systems, and services, the buyer must forge a compromise by asking some variation of the question: What drop in quality is acceptable, and at what price? The nature of structural optimization is the same: what quality of structural system can be accepted given its price. This quandary can be stated within a PBSD framework as seeking an optimized seismic design that achieves a balanced minimization of two (or more) general competing objectives which are monetary investment and seismic risk (Liu, Burns, & Wen, 2005). A "balanced minimization" is a solution that does not disproportionately sacrifice one competing objective in favor of the other, but rather a solution that has been arrived at by compromising equally on both objectives. An ideal methodology would not only find a set of agreeable solutions but would also produce a tool that that could be used to evaluate the tradeoffs between solutions and form a

basis of decision making (Foley et al., 2007). Such tools could be brought to owners and other stakeholders and would allow them to make informed decisions, not only about the level of risk they are willing to accept but also, specifically, how much money that risk could end up costing. Thus the appeal of adding an optimization procedure to a design/analysis routine: actual, probability based hard cost data that directly reflect the consequences of various design decisions.

3.2 Solution Engines

As exciting as the results of a well-founded structural optimization procedure may be, the actual execution of such a procedure is no easy task. Effective optimization procedures are highly iterative and involve the trial of perhaps thousands of different design alternatives. Not only must sufficiently random design alternatives be generated, each and every alternative must be fully analyzed to check for performance objective compliance. The computational burden of such a procedure is, in simple practical terms, entirely beyond the ability of an individual. As such, algorithms have been developed that efficiently execute the steps necessary to execute a meaningful optimization procedure. These algorithms, termed either Genetic Algorithms or Evolutionary Strategies, are the subject of the next sections.

3.2.1 Genetic Algorithms

A set of optimum solutions that have been reached by exhausting all (or a great many) of the possible solutions is desired. Additionally, the optimization scheme should reflect the probabilistic nature of performance critical to the foundation of PBSD philosophy. Genetic algorithms, in use since the 1960s, are solution engines by which the desired results can be achieved. Genetic algorithms are search and optimization engines that are able to consider multiple objectives both simultaneously and separately using the survival of the fittest principle common in the biological sciences. GAs have been widely and effectively utilized in a broad range of engineering applications. They are particularly valuable because of their ability to handle discrete valued design variables without trouble. This ability is particularly critical when we consider the optimization of a steel moment resisting frame. The ability to handle discrete valued design variables means that GAs are able to handle the standard commercially available rolled steel sections and their respective properties. Additionally, because genetic algorithms are

able to maintain a large number of solutions concurrently, a wide distribution of optimized solutions can be obtained by running the algorithm a single time (Liu, Burns, & Wen, 2006).

Gaining insight into how GAs work is important for understanding the nature of their results. They operate on solutions that are built onto chromosomes, or genotypic representations, from their original data values, which are termed phenotypic representations. These representations are illustrated graphically in Figure 3.2.1-1.

Figure 3.2.1-1 Graphical Representation of GA Chromosomes

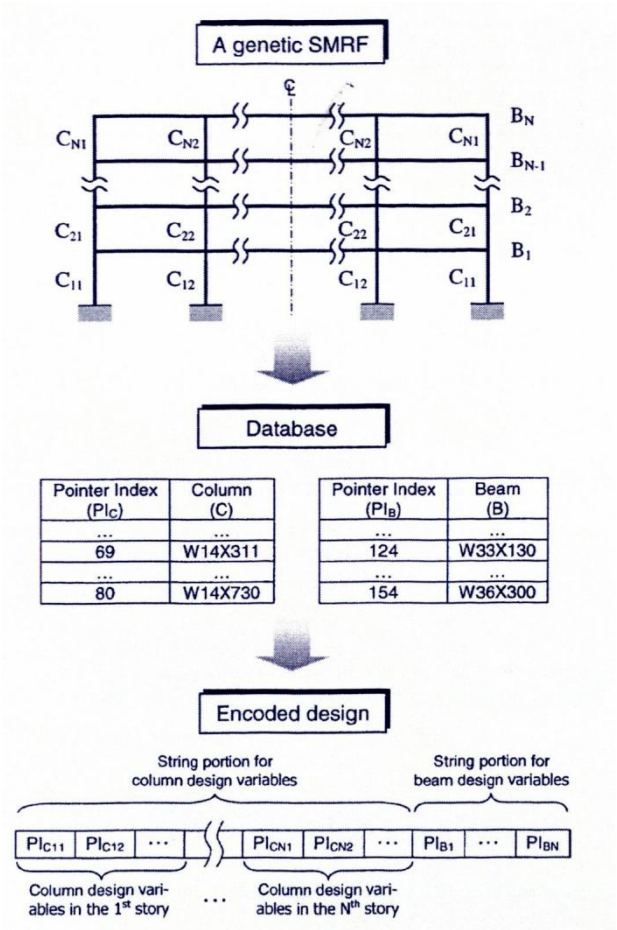

Source: Liu, M., & Burns, S., & Wen, Y. (2006, January). Genetic algorithm based construction-conscious minimum weight design of seismic steel moment-resisting frames. *Journal of Structural Engineering*, 50-58.

These chromosomes decode to the configurations and section properties of the individual members that compose the frame or frames. GAs begin their run from an initial set of possible solutions, termed a population, that are randomly made. The size and treatment of this initial population is an important component in setting up an efficient run. Taking the current (initial, at this point) population, each solution is evaluated for the pre-defined objective functions and its

relative merit within the population is measured by a fitness value. The individual fitness value of each of the population solutions is evaluated and the solutions with the best (highest) fitness values are chosen by the GA using a selection operation. The selected solutions are used to populate a new mating pool. The second unique GA operation, crossover, is executed on the solutions in the new mating pool. In a crossover operation, two parent solutions in the mating pool are selected at random and their respective data values interchanged based on a prescribed crossover probability. The new solutions resulting from the crossover operation are termed, not surprisingly, offspring. The purpose of the crossover operation is, hopefully, to effectively breed a better generation of solutions by randomly recombining the best attributes of the generation of solutions previous. Next, the third unique GA operation is executed: mutation. Mutation is a process by which the chromosome value of an offspring solution at one or more randomly selected locations is changed according to a predefined mutation probability. The goal of the mutation operation is to introduce new variability in the procedure that may not be discovered using crossover and selection procedures. Increasing variability helps to unleash new solution possibilities and increase the likelihood of reaching the best possible solution. After all three basic operations have been completed, an entirely new solution generation, derived from the initial population, has been reached. The execution of the GA consists of a repetition of this process until a predefined termination condition is reached. Examples of termination conditions are when the maximum number of generations has been reached or when the improvement between consecutive optimized solution generations is negligible (Liu et al., 2006).

Because the optimization problems faced within a PBSD context are almost always multi-objective in nature, we must define a single measure of merit that can be extended to describe the relative merit of all solutions taking into consideration all relevant objectives. The measure of merit is termed a fitness measure and the method for applying this fitness measure is termed the nondominating sorting technique. The nondominating sorting technique is a procedure in which all solutions in a population are ranked. Considering any given population, a solution is dominated if there is another solution in that same population that is better in at least one objective and no worse in all others. All solutions in a population that are not dominated are considered a nondominated subset. The nondominated subset solutions are each assigned a rank of one and then, for the time being, removed from the population. The next collection of solutions that are not dominated are grouped into another nondominated subset, assigned a rank

of two, and again temporarily deleted from the population. This process continues until each member of the population has been assigned a rank number. The lower number the rank, the higher the fitness (Liu et al., 2006). Thus, solutions within the populations given a rank of one are considered the fittest, or best considering the objectives at hand, solutions, pending future generations. In this way we are able to assign every solution in the population a relative rank of merit that simultaneously considers all objectives.

The final component that will solidify our understanding of the nature of genetic algorithms is the concept of elitism. An elitist is the best possible solution in a single generation. Elitists are usually the nondominated solutions – having a rank of one – for a given generation. Given this high level of merit, it is desirable that elitists are kept from generation to generation such that their properties can be spread to other candidate solutions using the three operations defined above. Given the random nature of the GA procedure, it is entirely possible that elitists may be accidentally corrupted or lost as the population passes from generation to generation. This is certainly undesirable and it has been shown that retention of elitist solutions is critical for improving the results of an optimization procedure. As such, it is generally proposed that a special procedure is added that will ensure the retention of GA solutions. One such procedure is to forcibly insert elitists from the previous generation back into the current, or offspring generation. This is done after the three basic operations have been performed. The GA then gathers an up-to-date list of elitists that includes those from the last generation as well as newly determined elitists within the first nondominated subset of the current generation (Liu et al., 2006). In this way, the best possible solutions are preserved from one generation to the next, which helps the overall procedure converge to the best possible solution as quickly as possible.

3.2.2 Evolution Strategies

An evolution strategies (ES) algorithm is another option for a multi-objective optimization problem solution engine. ESs are similar to GAs and many of the topics introduced above can be applied here as well. In particular, ESs also use the same three basic nondeterministic operators: selection, mutation, and crossover (or recombination). In addition, both solution engines are able to work simultaneously with a large population of design points. However, a notable difference between the two is that ESs reach a higher rate of convergence

and generally are considered more efficient than GAs for solving real world problems (Papadrakakis, Lagaros, Thierauf, & Cai, 1998).

The first notable difference between the ES and GA is in the fashion in which the ES runs the mutation operation. Mutation, which is enacted within one generation rather than between two generations, is best described by a probability distribution in which small changes happen frequently but large changes occur only rarely. The difficulty in effectively coding this desired behavior lies in determining what is known as the step length. Step lengths that are too small cause the algorithm to become inefficient and run an unnecessarily large number of iterations. Conversely, if the step length is too large, the procedure will never meaningfully converge to the solution. The solution to this problem, a self-adapting search mechanism, plays a large part in making the ES more efficient than the GA. Built into the ES algorithm is the rule that 20% of all mutations should be successful mutations (Papadrakakis et al., 1998). Additionally, constraints can be placed within the algorithm that will either increase or decrease this proportion as necessary at intervals (i.e. number of mutations) defined by the analyst. ES procedures can be continuous or discrete in nature. As indicated previously, it is generally more desirable in the context of structural optimization, and particularly for the optimization of steel structures, to deal with variables in a discrete fashion. For this case, the mutation vector does not change all components of the previous solution, but will randomly change only a few at each execution of the mutation operator. For continuous cases, the mutation operator carries a possibility that all components will be changed each time but usually only by a small amount (Papadrakakis et al., 1998). In certain instances, particularly in the case of reinforced concrete structures, the use of a continuous ES may be useful.

Finally, we should keep in mind that there are two different types of ES. The first is $(\mu+\lambda)$-ES and the second is (μ,λ)-ES where μ corresponds to the parent solutions that will produce λ offspring. In the first case, the best μ individual solutions are chosen from a temporary population of parent and offspring solutions to form the parents of the next generation. In the second case, the μ individuals produce λ offspring, where there are fewer μ than λ, and the selection operation creates a new population of μ individual solutions from the pool of λ offspring only. Thus, in the first case the life of each individual is not limited to a single generation, while in the second the life of each individual solution will last only one

generation (Papadrakakis et al., 1998). Choosing between the two options is mostly a matter of individual preference, though if there is any advantage a slight one rests with the (μ+λ)-ES type.

In either case, and in GAs as well, the numbers of parents and offspring, or the size of the population, has a large impact on the overall computational efficiency of the algorithm. In fact, the purposed advantage of a very large data base is, in the sense of producing the best quality final design, "practically not exploitable" (Fragiadakis & Papadrakakis, 2008). This is due to the fact that extremely large populations confuse the optimizer because the huge breadth of solutions does not allow the algorithm to explore a sufficient depth of possible solutions. The result is that the optimizer becomes confined in a cycle of repetitive, probably purposeless structural analyses that is incapable of producing a final result of acceptable quality. An enhancement to the standard algorithm that will solve this problem is multi-database cascade optimization. Cascading allows the analyst to split the initial large population into several smaller populations by deactivating some entries. This way, several coarser data bases are constructed and all possibilities of the initial large database are preserved. The individual populations are considered by the optimizer in successive stages and information between successive stages is shared. This means that when each individual population has gone through the optimization procedure, the sub-populations are recombined and new sub-populations are created, again by deactivating some entries. In this way, each step of the cascading process yields denser solutions and the procedure can still converge to a high quality final result (Fragiadakis & Papadrakakis, 2008).

3.2.3 Pareto Fronts

A final, very useful addition to either a GA or ES process is to include the development of an optimal Pareto front. Pareto fronts are graphical tools that can be used to illustrate the distribution of a set of solutions. Most often, Pareto fronts are drawn from the individual points comprising the highest ranked nondominated subset (elitists) of the current generation. These solution points are plotted according to their respective ordinate values on a coordinate plain, the axes of which correspond to the objectives being pursued. Because the highest degree of minimization possible for each objective is sought, the origin of this defined plain, termed objective space, represents the best possible solution (though we should keep in mind that simultaneous total minimization is not actually possible). Therefore, solutions closest to the

origin are the best, or fittest, solutions. While this sounds neatly organized, the actual output of elitist solutions plotted in objective space is anything but, as the solution points form a scattered "cloud" of possibilities. We need a way to summarize the solution cloud into a decision-making curve so that the trade-offs between adjacent designs can clearly be seen. The best way to accomplish this is to draw a Pareto front (Foley et al., 2007).

A Pareto front should indicate the fitness of individual solution points such that solutions closer to the origin have higher fitness and populations with higher fitness should have greater dispersion in objective space (Foley et al., 2007). The first Pareto front objective is transparent, but the second deserves some elaboration. It is preferable that our final population of optimized solutions takes into account the full range of possibility. As the optimization procedure progresses, there will invariably be give and take between competing solutions, the result of which will be that some solutions are better suited to satisfying Objective A over Objective B, and vice-versa. In terms of objective space, this is the equivalent of saying that some solutions will hew more closely to one axis than to the other. In order to capture this output behavior, it is important that the Pareto front is wide, in the sense that it extends from axis to axis and includes all the solutions, including those that have leaned closer to satisfying one objective over the other. The opposite of this is termed clustering, and is to be avoided for the sake of diversity of solutions. One option to avoid clustering is to include a coefficient in the objective statement that forces the GA or ES to keep moving along the Pareto front (Rojas, Pezeshk, & Foley, 2008). Thus, we are able to arrive at a solution with a wide range of solutions all of which fall on the same Pareto front optimality curve.

We now consider how to construct an effective Pareto front using the radial fitness formulation for two arbitrary competing design objectives, A and B, where A and B represent the axes that bound the objective space. We can define the location of the Pareto front curve based on a position vector defined as (Foley et al., 2007):

$$R_i = \sqrt{(A_{max} - A_i)^2 + (B_{max} - B_i)^2} \qquad \text{Equation 3.3.3-1}$$

Here, A_{max} and B_{max} are ordinates that define some solution point C, which itself represents the solution within the population that is the greatest distance from the origin. The radial distance of the ith solution, then, is merely the distance separating the worst design from the design considered, where the design considered is described by its ordinates A_i and B_i. Therefore, the optimal Pareto front for a given population, a population drawn from the nondominated subset, is

defined by minimizing the quantity 1/R for all solution points (Foley et al., 2007). The curve then defined by the radial distance satisfying the 1/R minimization constraint is the optimal Pareto front. This principle is illustrated graphically in Figure 3.2.3-1. Developing the Pareto front curve simplifies the cloud of solutions into a single curve that can easily be used to make decisions regarding design trade-offs.

Figure 3.2.3-1 Sample Optimal Pareto Front Curve

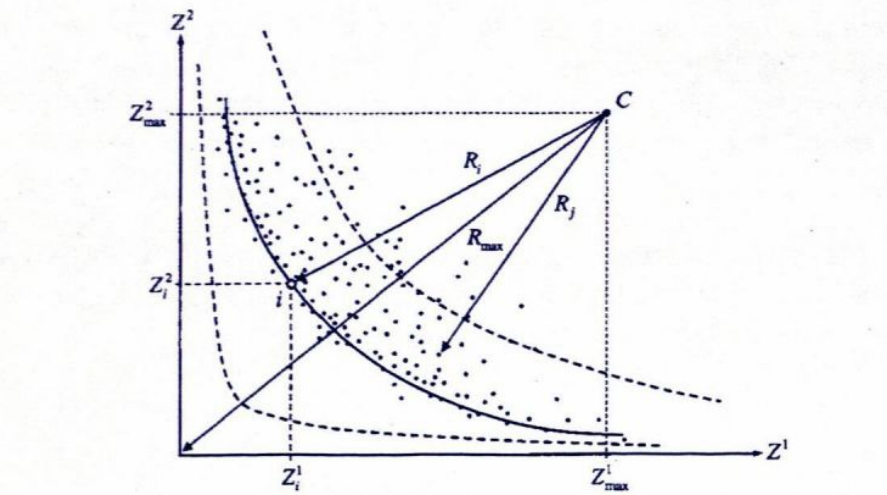

Source: Foley, C., & Pezeshk, S., & Alimoradi, A. (2007, June). Probabilistic performance-based optimal design of steel moment-resisting frames. I: Formulation. *Journal of Structural Engineering,* 757-766.

Objective space will be of the same dimension as the quantity of objectives pursued. Thus, objective space will be two dimensional for two competing objective functions, three dimensional for three competing objective functions, and so forth. While this can become spatially complex, the same procedure for defining the Pareto front can be used.

3.2.4 Execution

Now that all relevant components for an optimization have been sufficiently defined, the process by which an optimization procedure is executed is considered. Among the tasks at hand are to generate a population of potential solutions, analyze these solutions, check constraints, generate offspring, analyze the new generation, check constraints, and repeat until the termination definition has been met. Clearly, two separate components make up the full procedure: an analysis routine and an optimization routine. The analysis routine may be the execution of any one procedure from the four general categories of analysis methods presented above. The optimization routine may utilize either of the algorithms already presented, and will

include the three basic operations as well as the generation of a Pareto front for fitness determination.

At each step in the optimization, it becomes necessary to halt the optimization program and extract the relevant data for use in an analysis program. The possible solutions generated by the optimization program are each evaluated by the analysis program for conformance with the predefined constraints. The relevant response data – that is, the constraint measures determined from analysis – is taken from the analytical output and used to compute the objective functions for each design. The objective functions are analyzed in order to assign appropriate fitness to each solution, and the optimization cycle begins again (Ganzerli, Pantelides, & Reavely, 2000). The analysis includes not only determination of response quantities but also to check frame capacity and determine if the possible solution developed by the algorithm is even feasible (Fragiadakis & Papadrakakis, 2008). In this way the overall routine progresses: generate possible design solutions, analyze those solutions, check fitness based on analysis results, and generate new possible design solutions using the three GA or ES operations. This procedure continues until the termination point, some options for which were mentioned previously, is reached. It is important to note that appropriate solutions take a good deal of time to find. In fact, throughout the literature it is common to see the optimization procedure enacted for up to 200 generations before an acceptable Pareto front is developed.

3.3 Objective Problem Formulation

The tools explored in the preceding sections are common to all optimization problems: a solution engine must be used to evaluate an objective function, while a Pareto front illustrates the trade-offs inherent in the solutions given by the solution engine. The aspect unique to each optimization procedure, the objective problem formulation, is now considered. An objective problem formulation is a statement that defines what objectives are being pursued, what behavioral constraints are being used to bound possible solutions, and what variables are being solved for. The purpose of this section is to examine the various objectives, constraints, and variables used in optimization procedures. By examining how and when they are implemented, the engineer can get a clear understanding as to the possibilities associated with structural optimization procedures.

3.3.1 Objectives

The four basic types of objective functions are: minimize initial cost, minimize damage cost or life cycle cost, maximize confidence levels, and minimize the level of damage. The discussion of each of these individually is the focus of the following sections. Throughout the optimization research literature, these four types of objective functions are regularly mixed and matched into various types of multi-objective optimization problems, depending on the driving goal of the engineer. Designers particularly concerned with the high rate of variance of earthquake hazard may prefer a more probabilistically driven optimization procedure, leading to a confidence level maximization objective. Those concerned with the trade-offs associated with present investment and future risk would want to consider an objective function that seeks to minimize either damage cost or life-cycle cost. A discussion of what each objective consists of and how they are stated for inclusion in the solution engine routine follows.

3.3.1.1 Initial Cost Minimization

The most common objective among structural optimization procedures is the minimization of initial cost. This objective is essentially always computed and its minimization is generally predicated upon the minimization of material weight. For steel structures, the weight to be limited would strictly be that of the steel members, while for reinforced concrete structures the weight considered would consist of both the concrete and reinforcing steel. Clearly, assuming that minimizing a structure's weight directly minimizes its overall cost is something of a crude assumption. However, while minimizing weight is not an exact prediction, it can be considered a good indicator of structural cost. Work has been done, notably by Liu, Burns, and Wen (2005), to expand the definition of initial cost so as to include the added cost of design complexity. Design complexity, for steel structures, can be roughly measured by the number of different standard sections used. Reducing design complexity, measured by reducing section sizes, reduces cost for four reasons: more connections can be duplicated; chance for erection error is reduced; fabrication processes can be simplified which leads to cost savings by increasing the number of assemblies that can be duplicated; and larger volumes of a single member size are more economical (Liu et al., 2006). For such an objective, the GA or ES groups the Pareto front solutions both in terms of initial cost and number of section types. The minimization of the number of section types thus does not exactly receive its own objective

function, but rather is included by appropriate sorting of the results. Another attempt to directly integrate complexity considerations into initial cost objective functions is (Alimoradi et al., 2004):

$$C_{initial} = \alpha W_{col} + \beta W_{beam} + \chi N_{conn} \qquad \text{Equation 3.3.1.1-1}$$

where $C_{initial}$ is total initial cost, α is the cost per pound of column members, β is the cost per pound for beam members, and χ is a cost multiplier for each connection at the beam ends. In this way, the cost of costly complex connections can be directly considered rather than approximated. More often, however, initial cost will be assumed to be directly proportional to the weight of the structure. Thus, the objective function formulation may not directly mention cost, but rather will seek to minimize weight, which for a steel structure may be written as (Foley et al., 2007):

$$C_{initial} \propto \sum_{i=1}^{N_{mem}} \rho_i A_i L_i \approx V_{col} + V_{beams} \qquad \text{Equation 3.3.1.1-2}$$

where ρ_i is the material weight density, A_i is the cross-sectional area of the member and L_i is length of the member, which can be similarly expressed as the total volume of columns and beams, as shown on the right side of the equation. As noted, initial construction cost for reinforced concrete structures must include the weight – and cost, by including an appropriate cost multiplier – of the concrete as well as the weight of the reinforcing steel (Ganzerli et al., 2000):

$$C = C_c V_c + C_s W_s \qquad \text{Equation 3.3.1.1-3}$$

where C_c is the cost per volume of concrete, V_c is the volume of concrete, C_s is the cost per weight of reinforcing steel, and W_s is the weight of the reinforcing steel. This fundamental equation can be expanded by explicitly stating the volumes and weights (Fragiadakis & Papadrakakis, 2008):

$$C = C_c + C_s = \sum_i^N w_c b_i h_i L_i + \sum_i^N w_s \, (A_{S1,i} + A_{S2,i}) L_i \qquad \text{Equation 3.3.1.1-4}$$

where w_c is the unit cost of concrete, w_s is the unit cost of steel, b_i and h_i are section dimensions of the members and L_i is that member's length, and $A_{1,i}$ and $A_{2,i}$ are the top and bottom reinforcement, respectively.

Minimization of initial cost is the most basic objective function. Achieving the lowest upfront cost is an easy sell to owners and stakeholders, though inclusion of a Pareto front with any of the remaining types of objective functions can illustrate to the same parties what trade-offs they are making by agreeing to the least expensive design alternative.

3.3.1.2 Damage Cost Minimization

Selection of damage cost – or limit state cost, as it is sometimes called – as an objective function requires that the analyst be able to directly relate structural response, due to anticipated earthquake hazard, to the amount of structural damage and the cost associated with that damage. Damage, or limit state, cost for the *i*th limit state has many individual components and could be expressed as (Lagaros & Fragiadakis, 2007):

$$C_{LS}^{i} = C_{dam}^{i} + C_{con}^{i} + C_{ren}^{i} + C_{inc}^{i} + C_{inj}^{i} + C_{fat}^{i} \qquad \text{Equation 3.3.1.2-1}$$

where C_{dam} is the damage repair cost, C_{con} is the loss of contents cost, C_{ren} is the loss of rental cost, C_{inc} is the income loss cost, C_{inj} is the cost of injuries, C_{fat} is the cost of human fatality. We may think of limit state cost as being divided into two areas: direct loss and indirect loss. The first two terms, C_{dam} and C_{con}, constitute the direct loss associated with earthquake damage, while the remaining four parameters quantify indirect monetary loss. Whether or not indirect cost is included, determining total expected damage cost can be a complex procedure. Two different ways to compute and analyze expected future damage cost are in terms of life cycle cost and in terms of equivalent annual losses (EAL).

Effectively computing expected limit state costs does not stop at estimating a cost per damage rate. Rather, the ability to predict the probability of experiencing a seismic event while also predicting the severity of that event must occur. In addition, the structure's ability to respond to both mild and severe events must be considered before the assigning costs to damage quantities can begin. Total expected limit state cost, including both direct and indirect costs, may be generally expressed as (Zou et al., 2007):

$$f_{LS} = \sum_{r=1}^{N_r} P_r L_r \qquad \text{Equation 3.3.1.2-2}$$

where P_r is the occurrence probability of an earthquake at the *r*th performance (or, equivalently, hazard level) level and L_r is the expected structural failure loss for the *r*th performance level. The occurrence probability for each performance level can be determined by referencing the probabilistic hazard levels and earthquake probabilities of exceedance given by FEMA 356 (2000).

Developing a procedure through which the expected structural failure loss can be computed is the first focus. To compute L_r, two things are required: express damage in terms of some response quantity, and define "damage" in discrete, quantifiable terms. Both tasks can be accomplished by pegging five discrete damage states to corresponding ranges of interstory drift.

The five discrete damage states, negligible, slight, moderate, extensive, and complete are respectively represented by the vector (Zou et al., 2007):

$$A = \{A_1, A_2, A_3, A_4, A_5\} \qquad \text{Equation 3.3.1.2-3}$$

and each damage state is defined by an ascending range of interstory drift values. Thus, qualitative damage states organized according to quantified levels of structural response have been introduced. Two helpful assumptions are made: first, direct damage cost is linearly related to initial material cost, and second that indirect damage cost can be estimated by the ratio of indirect loss to direct loss for each of the five damage states. Sample values for determining damage state and structural loss are shown in Table 3.3.1.2-1.

Table 3.3.1.2-1 Damage States and Associated Losses

State of Damage	Negligible	Slight	Moderate	Severe	Complete
Interstory Drift (%)	< 1.0	1.0 - 2.0	2.0 - 4.0	4.0 – 10.0	> 10.0
Ratio of Direct Loss to Initial Material Cost	0.02	0.10	0.30	0.70	1.00
Ratio of Indirect Loss to Direct Loss	0.0	0.0	1.0 – 10.0	10.0 - 50.0	50.0 – 200.0

Source: Zou, X., & Chan, C., & Wang, Q. (2007, October). Multiobjective optimization for performance-based design of reinforced concrete frames. *Journal of Structural Engineering*, 1462-1473.

By making these assumptions, it will be possible to express both direct and indirect losses in terms of a structural response parameter, interstory drift in this case. These assumptions can be mathematically expressed as (Zou et al., 2007):

$$L_r(A) = \left[\sum_{q=1}^{5} \tilde{L}_q(A_q)\right] f_{initial} \qquad \text{Equation 3.3.1.2-4}$$

which should be evaluated for each of the *r* performance levels being considered. $\tilde{L}_q$ is the total direct and indirect structural damage loss corresponding to one of the five discrete damage states, A_q, and $f_{initial}$ represents the total initial material cost. Finally, by utilizing the indexed values of interstory drift used to define each discrete damage state, the total expected structural failure loss for each of the *r* performance levels can be expressed in terms of the *j*th interstory drift, τ_j, by (Zou et al., 2007):

$$L_r(\tau_j) = \left[\sum_{q=1}^{5} \mu_q(\tau_j)\tilde{L}_q\right] f_{initial} \qquad \text{Equation 3.3.1.2-5}$$

where $\mu_q(\tau_j)$ is a membership function relating the interstory drift at each of *j* stories to the five discrete damage level index values. This expression of L_r is then incorporated into the

expression for f_{LS} given above to determine the total structural damage cost associated with exceeding a certain damage state.

By utilizing the equations given and appropriate tabulated values, the total expected value of structural loss due to seismic hazard can be expressed as a fraction of initial cost. Thus, a useful decision making curve could be generated: initial material cost versus damage repair cost. However, the probabilistic nature of this method is ill-defined. The expected damage cost is conditional only on a single earthquake: the earthquake with intensity corresponding to the probability of occurrence in fifty years associated with a given performance objective. The damage cost computed therefore corresponds to a quite narrow range of possibilities, in terms of seismic hazard, and places the cost as occurring merely at some point over the course of fifty years. While this can be a useful method, perhaps a more useful output would quantify cost in terms of yearly probability over the life of the structure.

A procedure for establishing the minimization of equivalent annual losses as an objective function begins much the same way as the damage cost formulation given above: five discrete damage states are defined according to corresponding ranges of interstory drift values. To take into account the random nature of earthquake hazard, we must compute the conditional probability of being in or exceeding one of the five damage states, *ds*, given any engineering demand parameter, *EDP*, by using the equation (Rojas et al., 2008):

$$P[ds|EDP] = \Phi\left[\frac{1}{\beta_{ds}} ln \frac{EDP}{\overline{EDP}_{ds}}\right] \qquad \text{Equation 3.3.1.2-6}$$

where $\overline{EDP}_{ds}$ is the median value of the *EDP* being considered, Φ is the normal cumulative distribution function, and β_{ds} is the lognormal standard deviation of the *EDP* and *ds* considered. The *EDP* in this case is interstory drift. Using this relationship, a time-based performance assessment can be used to determine EAL. A time-based performance assessment is "an estimate of the probable earthquake loss, considering all potential earthquakes that may occur in a given time period, and the mean probability of the occurrence of each" (Rojas et al., 2008).

Using the probability distribution computed above, the total expected losses due to a given *EDP* can be computed as a percentage of building replacement cost (Rojas et al., 2008):

$$E[L_T|EDP] = \sum_{j=1}^{5} P[DM = ds_j \,|EDP] RC_{ds_j} \qquad \text{Equation 3.3.1.2-7}$$

where $P[DM=ds_j|EDP]$ is the probability that the damage measure will be equal to damage state *j* given a defined *EDP*, RC_{ds_j} is the repair cost due to damage state *j*. The probability that the

damage measure will be equal to a given damage state for a defined *EDP* and the repair cost ratio due to damage state *j* can be determined using HAZUS fragility functions. This procedure is repeated for each *EDP* of concern at each hazard level under consideration. The equations so far given can be used to construct loss curves that give the probability of loss that would result from seismic events exhibiting a given intensity and return period.

Because the objective is to summarize and describe losses on an annual basis due to all potential earthquakes, the estimated losses from each hazard level must be aggregated. Aggregating these losses yields an annualized loss curve which is described by the equation (Rojas, et al., 2008):

$$P[L_T > l] = \int_{\lambda} (1 - P[L_T \leq l|IM])d\lambda(IM) \approx \sum_{i=1}^{n}(1 - P[L_T \leq l|IM_i])\Delta\lambda(IM_i)$$ Equation 3.3.1.2-8

where $(1 - P[L_T \leq l|IM_i])$ is the probability of loss exceeding *l* for an earthquake with intensity *IM*, $\Delta\lambda(IM_i)$ is the mean annual recurrence interval of a given ground motion intensity, and *n* is the number of hazard levels considered. By integrating the area under the curve drawn by the preceding equation, we arrive at the EAL as a percentage of building cost. This point is illustrated in Figure 3.3.1.2-1.

Figure 3.3.1.2-1 Equivalent Annual Loss Curve

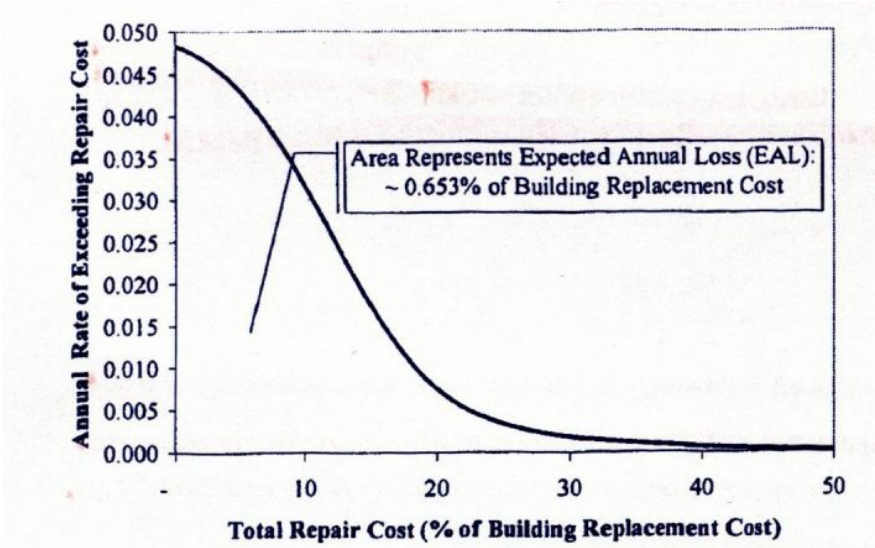

Source: Rojas, H., & Pezeshk, S., & Foley, C. (2008, April). Automated risk-based seismic design method for optimal structural and non-structural system performance. *Crossing Borders Structures 2008 Structures Conference*.

By implementing the EAL objective function into a multi-objective optimization procedure with minimization of initial weight as the competing objective, a Pareto front curve may be drawn to compute a return on investment (ROI) between two competing solutions. The

objective space for an EAL versus initial weight scenario would have EAL on the abscissa and initial weight on the vertical axis. Then, the horizontal distance between any two solutions would be the difference in annual benefit while the vertical distance between the same two solutions would be the additional initial cost. Thus, by dividing annual benefit by the difference in initial cost we can compute the ROI for two alternative solutions (Rojas et al., 2008). Put another way, ROI is equal to the inverse of the linear slope between any two solution points in objective space. Return on investment is a very powerful decision making tool and can put design decisions before owners and stake holders in the most effective manner to make trade-off design decisions.

3.3.1.3 Confidence Maximization

The third alternative for objective formulation is to require that confidence in structural response, for a presumed earthquake loading, is at its maximum level. While FEMA documents state minimum levels of confidence that must be achieved for corresponding performance objectives, engineers prefer to be as confident as possible that the design is sufficiently able to resist the design loading - a certain level of damage will not be exceeded. By comparing confidence to cost, for example, more expensive designs also have higher levels of confidence associated with their performance, and vice-versa. In this way the engineer can provide owners and stakeholders with analytical information concerning the level of risk they are willing to accept. The simplest way to state a confidence objective function is to minimize (Alimoradi et al., 2004):

$$F = \frac{1}{q^{IO}} \qquad \text{Equation 3.3.1.3-1}$$

where q^{IO} is the confidence level associated with the Immediate Occupancy performance objective. By seeking to minimize the inverse of the confidence level we can stay consistent with the other types of objective functions, all of which aim to minimize rather than maximize their respective parameters. Obviously, multiple confidence level objective functions could be stated and implemented, one for each performance objective being pursued.

Another way to consider confidence in performance as an objective is to pursue what is termed a “balanced design” objective (Foley et al., 2007). This type of objective formulation is only useful when two different response parameters are being used to judge conformance with the chosen performance objectives. An example pair would be interstory drift and column

compression force for steel moment frames. The aim of a balanced design objective is to ensure that the confidence levels associated with each response parameter of interest are high and as close in value as possible. Trying to match confidence levels is a boost towards economical designs as doing so would prevent one response parameter from overwhelmingly dominating the design requirements. For the two example response parameters given above, a balanced design objective formulation may take the form of (Foley et al., 2007):

$$F = \frac{(q_{CCF}^{IO} - q_{ISD}^{IO})^2}{q^{IO}} \qquad \text{Equation 3.3.1.3-2}$$

where minimizing the foregoing equation is the objective. The formulation seeks to maximize overall confidence, q^{IO}, while simultaneously minimizing the difference in confidence levels between column compression force and interstory drift. Accomplishing both tasks would minimize the objective function, F. Again, similar objective functions could be written for other performance objectives and other response parameters.

Maximizing confidence is analogous to minimizing risk which itself is analogous to minimizing the variance of the structural response given the many uncertainties inherent in any earthquake engineering problem. Another way to minimize risk is to attempt to minimize the standard deviation of the response, σ_{resp}. Response deviation minimization is undertaken with the additional consideration that both the ground motion excitation and the structural material properties are random variables (Lagaros & Fragiadakis, 2007). For this procedure, the mean spectrum and standard deviation of the expected ground motion are used to describe the structural demand. Treating the design process as a statistical distribution of both capacity and demand possibilities, standard deviation acts to describe the level of certainty of the analytical output. Minimizing uncertainty also minimizes risk, and can be used effectively to make informed design trade-off decisions.

3.3.1.4 Damage Minimization

As a simpler alternative, it may be advisable to strictly focus on limiting some response parameter that is indicative of structural damage, without necessarily computing a corresponding damage cost. Response parameters that are good indicators of structural damage are interstory drift and plastic hinge rotation. In particular, limiting a damage response parameter may be useful if the response parameter takes on a global, rather than a local, structural significance. This statement is driven by the observation that formation of a soft story and the subsequent

disproportionate accumulation of plastic deformation is a common cause of structural collapse (Grierson et al., 2006). Designing a structure to drift uniformly over its height would remove the threat of soft story development, and therefore the pursuit of uniform interstory drift over the height of a structure is considered an erstwhile objective for preventing global structural damage. This objective may be stated as (Grierson et al., 2006):

$$f(x) = [\frac{1}{n_s}\sum_{s=1}^{n_s-1}(\frac{v_s^{CP}(x)\div H_s}{\Delta^{CP}(x)\div H} - 1)^2]^{1/2} \qquad \text{Equation 3.3.1.4-1}$$

where n_s is the number of stories, v_s^{CP} and Δ^{CP} are the drift story s and the roof drift at the collapse prevention hazard level, respectively, H_s is the vertical distance from the base of the structure to story s, and H is the height of the structure. A structure with perfectly uniform drift would result in the function $f(x)$ being equal to zero. The function essentially defines the coefficient of variation for the lateral drift of the structure. Minimizing the lateral drift variation ensures that the difference in drift over the height of the building is as uniform as possible, thereby equitably distributing damage over the height of the building and preventing excessive damage concentration.

3.3.2 Constraints

While the objective functions define the types of solutions the algorithm will pursue, constraints act to eliminate unsatisfactory designs as the algorithm progresses. Constraints take several forms, but always act to limit solutions by disallowing undesirable behavior. They generally establish minimums that will not be violated in much the same fashion as design codes and manuals. That is, they establish baselines that ensure a desired outcome. Constraint statements within an optimization routine take one or more of the following forms: confidence constraints, response constraints, member constraints, and code-based constraints.

3.3.2.1 Confidence Constraints

For all performance objectives FEMA documents have established minimum levels of confidence that must be met to ensure a reasonable level of reliability in the outcome predicted. Confidence constraints explicitly state these minimums within the algorithm. They may be formulated as (Alimoradi et al., 2004):

$$0.50 - q^{IO} \leq 0.0 \qquad \text{Equation 3.3.2.1-1}$$

which could be expanded to include confidence levels for other performance objectives. The minimum confidence level for Immediate Occupancy performance established by FEMA is 50%, and the above constraint statement ensures this result for all solutions. Alternatively, the confidence constraint statement could be simplified to (Foley et al., 2007):

$$q^{IO} \geq q_{limit}^{IO} \quad \text{Equation 3.3.2.1-2}$$

where the limit confidence level is defined by the analyst according to FEMA specifications. Whatever the exact formulation used, implementing confidence constraints will force the algorithm to produce only solutions that meet minimum confidence level standards.

3.3.2.2 Response Constraints

For any type and material of lateral force resisting system, FEMA 356 (2000) defines limit state response values that are used to delineate between performance objectives. These response parameters usually take the form of interstory drift values or plastic member rotations. In either event, when we are designing a structure with the aim of achieving, say, Immediate Occupancy performance, the only way to verify meeting Immediate Occupancy performance is by meeting the interstory drift requirements stated in FEMA 356 (2000). Therefore, an often used constraint is to place maximum boundaries on interstory drift. Just as with confidence constraints, response constraints force the algorithm to discard solutions whose interstory drift values exceed the maximum for a given performance level. An example of this formulation is (Grierson et al., 2006):

$$\delta_s^i(x) \leq \bar{\delta}^i \quad (i = 1, \dots, n_h; s = 1, \dots, n_s) \qquad \text{Equation 3.3.2.2-1}$$

where δ_s^i is the interstory drift at level *s* due to the *i*th hazard level, $\bar{\delta}^i$ is the allowable interstory drift due to the *i*th hazard level, n_h is the number of earthquake hazard levels being concerned and n_s is the number of levels in the structure. Similar statements could be written for other response parameters.

3.3.2.3 Member Constraints

Member constraints are most often implemented when reinforced concrete systems are being optimized. This is due to the considerations that come into play when one seeks to optimize the quantity of steel reinforcing within each member. Not only must the reinforcement ratios conform to code values, the amount of steel required by the optimized solution must actually be able to physically fit, including clearance requirements, in the concrete members.

The first of these concerns may be met by bounding the steel reinforcement ratio, ρ, by its minimum and maximum code specified quantities considering the type of member (beam or column) as well as both tensile and compressive reinforcement. The second concern can be handled by writing a statement similar to (Fragiadakis & Papadrakakis, 2008):

$$b - (2c + n_b \emptyset + (n_b - 1) \times \max(1", \emptyset) \geq 0 \qquad \text{Equation 3.3.2.3-1}$$

where b is the width of the member, n_b is the number of bars, c is the concrete cover and $\emptyset$ is the diameter of the bars. Thus, required clearances are explicitly integrated into the rebar optimization process and we can be assured that the designed quantities of steel will be able to fit within the designed member sizes.

3.3.2.4 Code-Based Constraints

Code-based constraints restrict solutions to commonly used minimum code requirements. The most common code-based constraint is to mandate adherence to strong-column weak-beam (SCWB) behavior. Other requirements within this category are usually based on member strengths and bending-axial force interaction behavior. Given the level of performance generally mandated by performance objectives in terms of drift and confidence, member strengths are usually not a factor. This being said, instituting code-based constraints are worthwhile in that they ensure that solutions not meeting minimum standards are rejected.

3.3.3 Variables

No matter what objective functions and constraints are used to define an optimization routine, the variables will always be the structural members themselves. Handling member sizes as variables varies depending on whether steel or reinforced concrete framing systems are used.

3.3.3.1 Steel Structures

Defining steel members as variables is considerably simpler compared to defining concrete members as variables. To simplify the optimization routine, it is best to minimize the number of variables used to describe the steel cross-sections. For example, by utilizing functional relationships obtained through regression analysis, each steel member can be defined merely by its cross-sectional area by (Grierson et al., 2006):

$$I = C_1 A^2 + C_2 A + C_3 \qquad \text{Equation 3.3.3.1-1}$$

$$S = C_4 A + C_5 \qquad \text{Equation 3.3.3.2-2}$$

$$Z = \varsigma S \qquad \text{Equation 3.3.3.2-3}$$

where C_1 through C_5 and ς are all determined by regression analysis. Thus, all possible steel members used in the various solutions will be individually and discretely determined and defined according to their cross-sectional area alone.

3.3.3.2 Reinforced Concrete Structures

Reinforced concrete structures are considerably more difficult in terms of defining each member's cross-sectional properties in terms of variables, as we must be able to optimize not only the concrete dimensions of each member but also the quantity of reinforcing steel within each member. The best way of dealing with this issue is to determine each separately. Knowing that longitudinal steel reinforcement is overwhelmingly responsible for a reinforced concrete structure's ability to respond in a ductile fashion during a severe seismic event, the optimization process can be broken into two phases. First, simple gravity loading and very mild earthquake forces are used to optimize the size of each concrete member cross-section. In the second phase, the cross-sections determined in the first phase are locked and more severe ground motions are used to determine the quantity of reinforcing steel, in terms of the reinforcement ratio, ρ, required (Zou & Chan, 2005). The objective function is then written in terms of ρ, which will yield the optimized design solutions based on reinforcement quantities for each member. A helpful assumption throughout this process is to presume that compression reinforcement is equal to tension reinforcement in columns and linearly related to tension reinforcement in beams. This way, only one variable must be solved for rather than two. For objective functions focused on limiting interstory drift and plastic hinge rotation, implementing the principle of virtual work is useful for rewriting the objective functions in terms of ρ. This process is intensive and lengthy, and the reader is referred to Zou and Chan (2005) for the full procedure.

All relevant components of a PBSD structural optimization procedure have now been identified. The examples cited for objective functions, constraints, and variables are not meant to represent the full extent of possibilities. Rather, they are meant to give the reader a frame of reference when considering the basic process of outlining an optimization procedure. Structural optimization is a widely applicable procedure that presents many different opportunities for customization for the problem at hand. The literature has presented a good variety of case studies, utilizing both steel and reinforced concrete structures, which have consistently shown the potential of optimization procedures in terms of their ability to make a significant impact as a

design tool. These procedures have been demonstrated to be logical and powerful extensions of the fundamental PBSD philosophy. Properly executed optimization procedures allow all involved parties to make informed trade-off decisions that help minimize seismic risk.

CHAPTER 4 - Summation

An explanation of the basic tenets of PBSD as well as analysis and optimization procedures that fit neatly into the PBSD framework has been presented. PBSD rests on the basic principle of minimizing structural damage cost while maximizing the engineer's confidence in structural performance. Taken together, these two aims amount to minimizing the risk associated with seismic hazard. The roadmap for any PBSD procedure begins with selecting either one or multiple performance objectives. Performance objectives are defined and constrained by quantitative structural response and level of seismic hazard. Though still at an early stage, PBSD methodology has been used in California for designing essential facilities, primarily hospitals. Additionally, PBSD has been applied on the West Coast in the case of sensitive data and manufacturing centers that would suffer huge indirect monetary losses should a seismic event interrupt normal business practice.

Assessing a structure's performance for comparison with the stated performance objectives is accomplished by using one of four broad categories of analysis procedures: linear static, linear dynamic, nonlinear static, and nonlinear dynamic. The degree of uncertainty associated with each category decreases from linear static to nonlinear dynamic, though at the cost of increased computational burden. Where applicable, several procedures were introduced that are well-suited to returning good quality results with significantly diminished computational effort. The procedures discussed do not constitute an exhaustive list of possible analysis procedures, but rather offer a representative sample of the wider population of all analysis procedure options. The analysis procedure ultimately used in a given PBSD procedure should be carefully selected to efficiently return reliable results without undue computational exertion. Where situations allow, particularly in cases where a building is geometrically regular and the natural period of vibration is sufficiently short, nonlinear static procedures are generally a better alternative to nonlinear dynamic procedure as the former is able to produce good quality results with far less associated effort than in the latter. The application of nonlinear dynamic procedures should be spared for situations where it is absolutely necessary, as when structural fundamental period is exceptionally long the structure presents numerous geometric, mass, and stiffness irregularities.

Finally, multi-objective optimization procedures were presented as a powerful extension to the basic goals of PBSD. The optimization procedures presented give an engineer an understanding of the incredible versatility of structural optimization. Though complex, the solution engines discussed are very workable endeavors that can have a huge impact on the final structural design. At this stage, optimization procedures are largely at an early stage in the sense that though their efficacy has been demonstrated in numerous academic works the real world application of multi-objective optimization procedures for structures is for the most part untested.

Performance-based seismic design is still a growing methodology. Ongoing research by academics and design professionals around the world is continually expanding the scope and capabilities of PBSD. As ever larger quantities of fruitful research are developed, the profile of PBSD within the structural engineering community will only increase. Therefore, a fundamental understanding of the component parts of the PBSD methodology is essential as engineering practice continues to evolve and improve. The information presented within this report has sought to establish this fundamental understanding. Going forward, a fundamental understanding of PBSD methodology will be a crucial base upon which to build as the implementation of PBSD procedures becomes more common.

References

Alimoradi, A., & Pezeshk, S., & Foley, C. (2004, May). Automated Performance-Based Design of Steel Frames. *Building on the Past, Securing the Future Proceedings of the 2004 Structures Conference*, 1429-1443.

Applied Technology Council. *Seismic Evaluation and Retrofit of Concrete Buildings*, ATC-40, Redwood City, CA, 1996.

Chopra, A. (2007). *Dynamics of Structures Theory and Applications to Earthquake Engineering*, Third edition, Pearson Prentice Hall.

Chopra, A., & Goel, R. (2002). A modal pushover procedure for estimating seismic demands for buildings. *Earthquake Engineering and Structural Dynamics, 31*, 561-582.

Farrow, K., & Kurama, Y. (2003). SDOF demand index relationships for performance-based seismic design. *Earthquake Spectra, 19*, 799-838.

Foley, C., & Pezeshk, S., & Alimoradi, A. (2007, June). Probabilistic performance-based optimal design of steel moment-resisting frames. I: Formulation. *Journal of Structural Engineering,* 757-766.

Fragiadakis, M., & Papadrakakis, M. (2008). Performance-based optimum seismic design of reinforced concrete structures. *Earthquake Engineering and Structural Dynamics, 37*, 825-844.

Freeman, S., & Paret, T., & Searer, G., & Irfanoglu, A. (2004, May). Musings on Recent Developments in Performance Based Design. *Building on the Past, Securing the Future Proceedings of the 2004 Structures Conference*, 725-736.

Ganzerli, S., & Pantelides, C., & Reavely, L. (2000). Performance-based design using structural optimization. *Earthquake Engineering and Structural Dynamics, 29*, 1677-1690.

Grierson, D., & Gong, Y., & Xu, L. (2006). Optimal performance-based seismic design using modal pushover analysis. *Journal of Earthquake Engineering, 10*, 73-96.

Gupta, A., & Kunnath, S. (2000). Adaptive spectra-based pushover procedure for seismic evaluation of structures. *Earthquake Spectra, 16*, 367-392.

Hamburger, R. (1997, January 31). *A Framework for Performance-Based Earthquake Resistive Design.* Retrieved September 12, 2007, from http://nisee.berkeley.edu/lessons/hamburger.html

Hasan, R., & Xu, L., & Grierson, D. (2002). Push-over analysis for performance-based seismic design. *Computers and Structures, 80,* 2483-2493.

Lagaros, N., & Fragiadakis, M. (2007). Robust performance-based design optimization of steel moment resisting frames. *Journal of Earthquake Engineering, 11,* 752-772.

Liu, M., & Burns, S., & Wen, Y. (2006, January). Genetic algorithm based construction-conscious minimum weight design of seismic steel moment-resisting frames. *Journal of Structural Engineering*, 50-58.

Liu, M., & Burns, S., & Wen, Y. (2005). Multiobjective optimization for performance-based seismic design of steel moment frame structures. *Earthquake Engineering and Structural Dynamics, 34*, 289-306.

McGuire, W., & Gallagher, R., & Ziemian, R. (2000). *Matrix Structural Analysis*, Second edition, John Wiley & Sons, Inc.

Newmark, N., & Hall, W. (1982). Earthquake spectra and design. Berkeley: Earthquake Engineering Research Institute.

Papadrakakis, M., & Lagaros, N., & Thierauf, G., & Cai, J. (1998). Advanced solution methods in structural optimization based on evolution strategies. *Engineering Computations, 15*.

Priestley, M. (2000). Performance-based seismic design. *Bulletin of the New Zealand National Society for Earthquake Engineering, 33,* 325-346.

Rojas, H., & Pezeshk, S., & Foley, C. (2008, April). Automated risk-based seismic design method for optimal structural and non-structural system performance. *Crossing Borders Structures 2008 Structures Conference*.

Ruiz-Garcia, J., & Miranda, E. (2007). Probabilistic estimation of maximum inelastic displacement demands for performance-based design. *Earthquake Engineering and Structural Dynamics, 36*, 1235-1254.

U.S. Federal Emergency Management Agency. (2005, June). *Improvement of Nonlinear Static Seismic Analysis Procedures, FEMA 440*. Washington, DC: U.S. Government Printing Office.

U.S. Federal Emergency Management Agency. (2000, November). *Prestandard and Commentary for the Seismic Rehabilitation of Buildings, FEMA 356*. Washington, DC: U.S. Government Printing Office.

U.S. Federal Emergency Management Agency. (2000, June). *Recommended Seismic Design Criteria for New Steel Moment-Frame Buildings, FEMA 350*. Washington, DC: U.S. Government Printing Office.

U.S. Federal Emergency Management Agency. (2000, April). *Action Plan for Performance Based Seismic Design, FEMA 349.* Washington, DC: U.S. Government Printing Office.

U.S. Federal Emergency Management Agency. (1997, October). *NEHRP Guidelines for the Seismic Rehabilitation of Buildings, FEMA 273*. Washington, DC: U.S. Government Printing Office.

Vamvatsikos, D., & Cornell, C. (2004, May). Applied incremental dynamic analysis. *Earthquake Spectra, 20,* 523-553.

Vamvatsikos, D., & Cornell, C. (2002). Incremental dynamic analysis. *Earthquake Engineering and Structural Dynamics, 31*, 491-514.

van de Lindt, J., & Pei, S., & Liu, H. (2008, February). Performance-based seismic design of wood frame buildings using a probabilistic system identification concept. *Journal of Structural Engineering,* 240-247.

Xue, Q., & Wu, C., & Chen, C., & Chen, K. (2008). The draft code for performance-based seismic design of buildings in Taiwan. *Engineering Structures, 30,* 1535-1547.

Zou, X., & Chan, C., & Wang, Q. (2007, October). Multiobjective optimization for performance-based design of reinforced concrete frames. *Journal of Structural Engineering*, 1462-1473.

Zou, X., & Chan, M. (2005). Optimal seismic performance-based design of reinforced concrete buildings using nonlinear pushover analysis. *Engineering Structures, 27*, 1289-1302.

Appendix A - Permissions

The images contained within this document were not created by the author and are used by permission of the entities cited in this section. Permissions are listed alphabetically by publisher.

ASCE Permissions

Permission is granted for you to reuse:

Foley, C., & Pezeshk, S., & Alimoradi, A. (2007, June). Probabilistic performance-based optimal design of steel moment resisting frames. I: Formulation. Journal of Structural Engineering. Figure 4, page 764.

Liu, M., & Burns, S., & Wen, Y. (2006, January). Genetic Algorithm Based Construction-conscious minimum weight design of seismic steel moment-resisting frames. Journal of Structural Engineering. Figure 1, page 54.

Rohas, H., & Pezeshk, S., & Foley, C. (2008). Automated risk based seismic design method for optimal structural and non-structural system performance. 2008 ASCE 18th Analysis and Computation Specialty Conference. Figure 2, page 7.

in your dissertation. Please add a full credit line to the material
being reprinted: With permission from ASCE.

Xi Van Fleet
Senior Manager, Information Services
Publication Division
American Society of Civil Engineers
1801 Alexander Bell Drive
Reston, VA 20191

(703) 295-6278-FAX

PERMISSIONS@asce.org

Elsevier Permission

ELSEVIER LICENSE
TERMS AND CONDITIONS

Dec 06, 2009

This is a License Agreement between andrew cott ("You") and Elsevier ("Elsevier") provided by Copyright Clearance Center ("CCC"). The license consists of your order details, the terms and conditions provided by Elsevier, and the payment terms and conditions.

All payments must be made in full to CCC. For payment instructions, please see information listed at the bottom of this form.

Supplier

Elsevier Limited
The Boulevard,Langford Lane
Kidlington,Oxford,OX5 1GB,UK

Registered Company Number

1982084

Customer name

andrew cott

Customer address

1605 humboldt

manhattan, KS 66502

License Number

2323350246780

License date

Dec 06, 2009

Licensed content publisher

Elsevier

Licensed content publication

Computers & Structures

Licensed content title

Push-over analysis for performance-based seismic design

Licensed content author

R. Hasan, L. Xu and D. E. Grierson

Licensed content date

December 2002

Volume number

80

Issue number

31

Pages

11

Type of Use

Thesis / Dissertation

Portion

Figures/table/illustration/abstracts

Portion Quantity

1

Format

Electronic

You are an author of the Elsevier article

No

Are you translating?

No

Order Reference Number

Expected publication date

Dec 2009

Elsevier VAT number

GB 494 6272 12

Permissions price

0.00 USD

Value added tax 0.0%

0.00 USD

Total

0.00 USD

Terms and Conditions

INTRODUCTION

1. The publisher for this copyrighted material is Elsevier. By clicking "accept" in connection with completing this licensing transaction, you agree that the following terms and conditions apply to this transaction (along with the Billing and Payment terms and conditions established by Copyright Clearance Center, Inc. ("CCC"), at the time that you opened your Rightslink account and that are available at any time at http://myaccount.copyright.com).

GENERAL TERMS

2. Elsevier hereby grants you permission to reproduce the aforementioned material subject to the terms and conditions indicated.

3. Acknowledgement: If any part of the material to be used (for example, figures) has appeared in our publication with credit or acknowledgement to another source, permission must also be sought from that source. If such permission is not obtained then that material may not be included in your publication/copies. Suitable acknowledgement to the source must be made, either as a footnote or in a reference list at the end of your publication, as follows:

"Reprinted from Publication title, Vol /edition number, Author(s), Title of article / title of chapter, Pages No., Copyright (Year), with permission from Elsevier [OR APPLICABLE SOCIETY COPYRIGHT OWNER]." Also Lancet special credit - "Reprinted from The Lancet, Vol. number, Author(s), Title of article, Pages No., Copyright (Year), with permission from Elsevier."

4. Reproduction of this material is confined to the purpose and/or media for which permission is hereby given.

5. Altering/Modifying Material: Not Permitted. However figures and illustrations may be altered/adapted minimally to serve your work. Any other abbreviations, additions, deletions and/or any other alterations shall be made only with prior written authorization of Elsevier Ltd. (Please contact Elsevier at permissions@elsevier.com)

6. If the permission fee for the requested use of our material is waived in this instance, please be advised that your future requests for Elsevier materials may attract a fee.

7. Reservation of Rights: Publisher reserves all rights not specifically granted in the combination of (i) the license details provided by you and accepted in the course of this licensing transaction, (ii) these terms and conditions and (iii) CCC's Billing and Payment terms and conditions.

8. License Contingent Upon Payment: While you may exercise the rights licensed immediately upon issuance of the license at the end of the licensing process for the transaction, provided that you have disclosed complete and accurate details of your proposed use, no license is finally effective unless and until full payment is received from you (either by publisher or by CCC) as provided in CCC's Billing and Payment terms and conditions. If full payment is not received on a timely basis, then any license preliminarily granted shall be deemed automatically revoked and shall be void as if never granted. Further, in the event that you breach any of these terms and conditions or any of CCC's Billing and Payment terms and conditions, the license is automatically revoked and shall be void as if never granted. Use of materials as described in a revoked license, as well as any use of the materials beyond the scope of an unrevoked license, may constitute copyright infringement and publisher reserves the right to take any and all action to protect its copyright in the materials.

9. Warranties: Publisher makes no representations or warranties with respect to the licensed material.

10. Indemnity: You hereby indemnify and agree to hold harmless publisher and CCC, and their respective officers, directors, employees and agents, from and against any and all claims arising out of your use of the licensed material other than as specifically authorized pursuant to this license.

11. No Transfer of License: This license is personal to you and may not be sublicensed, assigned, or transferred by you to any other person without publisher's written permission.

12. No Amendment Except in Writing: This license may not be amended except in a writing signed by both parties (or, in the case of publisher, by CCC on publisher's behalf).

13. Objection to Contrary Terms: Publisher hereby objects to any terms contained in any purchase order, acknowledgment, check endorsement or other writing prepared by you, which terms are inconsistent with these terms and conditions or CCC's Billing and Payment terms and conditions. These terms and conditions, together with CCC's Billing and Payment terms and conditions (which are incorporated herein), comprise the entire agreement between you and publisher (and CCC) concerning this licensing transaction. In the event of any conflict between your obligations established by these terms and conditions and those established by CCC's Billing and Payment terms and conditions, these terms and conditions shall control.

14. Revocation: Elsevier or Copyright Clearance Center may deny the permissions described in this License at their sole discretion, for any reason or no reason, with a full refund payable to you. Notice of such denial will be made using the contact information provided by you. Failure to receive such notice will not alter or invalidate the denial. In no event will Elsevier or Copyright Clearance Center be responsible or liable for any costs, expenses

or damage incurred by you as a result of a denial of your permission request, other than a refund of the amount(s) paid by you to Elsevier and/or Copyright Clearance Center for denied permissions.

LIMITED LICENSE

The following terms and conditions apply only to specific license types:

15. **Translation**: This permission is granted for non-exclusive world **English** rights only unless your license was granted for translation rights. If you licensed translation rights you may only translate this content into the languages you requested. A professional translator must perform all translations and reproduce the content word for word preserving the integrity of the article. If this license is to re-use 1 or 2 figures then permission is granted for non-exclusive world rights in all languages.

16. **Website**: The following terms and conditions apply to electronic reserve and author websites:
Electronic reserve: If licensed material is to be posted to website, the web site is to be password-protected and made available only to bona fide students registered on a relevant course if:
This license was made in connection with a course,
This permission is granted for 1 year only. You may obtain a license for future website posting,
All content posted to the web site must maintain the copyright information line on the bottom of each image,
A hyper-text must be included to the Homepage of the journal from which you are licensing at http://www.sciencedirect.com/science/journal/xxxxx or the Elsevier homepage for books at http://www.elsevier.com , and
Central Storage: This license does not include permission for a scanned version of the material to be stored in a central repository such as that provided by Heron/XanEdu.

17. **Author website** for journals with the following additional clauses:

All content posted to the web site must maintain the copyright information line on the bottom of each image, and he permission granted is limited to the personal version of your paper. You are not allowed to download and post the published electronic version of your article (whether PDF or HTML, proof or final version), nor may you scan the printed edition to create an electronic version,
A hyper-text must be included to the Homepage of the journal from which you are licensing at http://www.sciencedirect.com/science/journal/xxxxx , As part of our normal production process, you will receive an e-mail notice when your article appears on Elsevier's online service ScienceDirect (www.sciencedirect.com). That e-mail will include the article's Digital Object Identifier (DOI). This number provides the electronic link to the published article and should be included in the posting of your personal version. We ask that you wait until you receive this e-mail and have the DOI to do any posting.
Central Storage: This license does not include permission for a scanned version of the material to be stored in a central repository such as that provided by Heron/XanEdu.

18. **Author website** for books with the following additional clauses:
Authors are permitted to place a brief summary of their work online only.
A hyper-text must be included to the Elsevier homepage at http://www.elsevier.com

All content posted to the web site must maintain the copyright information line on the bottom of each image
You are not allowed to download and post the published electronic version of your chapter, nor may you scan the printed edition to create an electronic version.

Central Storage: This license does not include permission for a scanned version of the material to be stored in a central repository such as that provided by Heron/XanEdu.

19. **Website** (regular and for author): A hyper-text must be included to the Homepage of the journal from which you are licensing at http://www.sciencedirect.com/science/journal/xxxxx. or for books to the Elsevier homepage at http://www.elsevier.com

20. **Thesis/Dissertation**: If your license is for use in a thesis/dissertation your thesis may be submitted to your institution in either print or electronic form. Should your thesis be published commercially, please reapply for permission. These requirements include permission for the Library and Archives of Canada to supply single copies, on demand, of the complete thesis and include permission for UMI to supply single copies, on demand, of the complete thesis. Should your thesis be published commercially, please reapply for permission.

21. **Other Conditions**: None

v1.6

Gratis licenses (referencing $0 in the Total field) are free. Please retain this printable license for your reference. No payment is required.

If you would like to pay for this license now, please remit this license along with your payment made payable to "COPYRIGHT CLEARANCE CENTER" otherwise you will be invoiced within 30 days of the license date. Payment should be in the form of a check or money order referencing your account number and this license number 2323350246780.
If you would prefer to pay for this license by credit card, please go to http://www.copyright.com/creditcard to download our credit card payment authorization form.

Make Payment To:
Copyright Clearance Center
Dept 001
P.O. Box 843006
Boston, MA 02284-3006

If you find copyrighted material related to this license will not be used and wish to cancel, please contact us referencing this license number 2323350246780 and noting the reason for cancellation.

Questions? customercare@copyright.com or +1-877-622-5543 (toll free in the US) or +1-978-646-2777.

John Wiley & Sons Permission

JOHN WILEY AND SONS LICENSE TERMS AND CONDITIONS

Dec 14, 2009

This is a License Agreement between andrew cott ("You") and John Wiley and Sons ("John Wiley and Sons") provided by Copyright Clearance Center ("CCC"). The license consists of your order details, the terms and conditions provided by John Wiley and Sons, and the payment terms and conditions.

All payments must be made in full to CCC. For payment instructions, please see information listed at the bottom of this form.

License Number	2323370380849
License date	Dec 06, 2009
Licensed content publisher	John Wiley and Sons
Licensed content publication	Earthquake Engineering and Structural Dynamics
Licensed content title	Incremental dynamic analysis
Licensed content author	Vamvatsikos Dimitrios, Cornell C. Allin
Licensed content date	Dec 19, 2001
Start page	491
End page	514
Type of Use	Dissertation/Thesis
Requestor type	University/Academic
Format	Electronic
Portion	Figure/table
Number of figures/tables	2
Original Wiley figure/table number(s)	Figure 6 Figure 7
Will you be translating?	No
Order reference number	
Total	0.00 USD
Terms and Conditions	

TERMS AND CONDITIONS

This copyrighted material is owned by or exclusively licensed to John Wiley & Sons, Inc. or one if its group companies (each a "Wiley Company") or a society for whom a Wiley Company has exclusive publishing rights in relation to a particular journal (collectively "WILEY"). By clicking "accept" in connection with completing this licensing transaction, you agree that the following terms and conditions apply to this transaction (along with the billing and payment terms and conditions established by the Copyright Clearance Center Inc., ("CCC's Billing and Payment terms and conditions"), at the time that you opened your Rightslink account (these are available at any time at http://myaccount.copyright.com).

Terms and Conditions

1. The materials you have requested permission to reproduce (the "Materials") are protected by copyright.

2. You are hereby granted a personal, non-exclusive, non-sublicensable, non-transferable, worldwide, limited license to reproduce the Materials for the purpose specified in the licensing process. This license is for a one-time use only with a maximum distribution equal to the number that you identified in the licensing process. Any form of republication granted by this licence must be completed within two years of the date of the grant of this licence (although copies prepared before may be distributed thereafter). Any electronic posting of the Materials is limited to one year from the date permission is granted and is on the condition that a link is placed to the journal homepage on Wiley's online journals publication platform at www.interscience.wiley.com. The Materials shall not be used in any other manner or for any other purpose. Permission is granted subject to an appropriate acknowledgement given to the author, title of the material/book/journal and the publisher and on the understanding that nowhere in the text is a previously published source acknowledged for all or part of this Material. Any third party material is expressly excluded from this permission.

3. With respect to the Materials, all rights are reserved. No part of the Materials may be copied, modified, adapted, translated, reproduced, transferred or distributed, in any form or by any means, and no derivative works may be made based on the Materials without the prior permission of the respective copyright owner. You may not alter, remove or suppress in any manner any copyright, trademark or other notices displayed by the Materials. You may not license, rent, sell, loan, lease, pledge, offer as security, transfer or assign the Materials, or any of the rights granted to you hereunder to any other person.

4. The Materials and all of the intellectual property rights therein shall at all times remain the exclusive property of John Wiley & Sons Inc or one of its related companies (WILEY) or their respective licensors, and your interest therein is only that of having possession of and the right to reproduce the Materials pursuant to Section 2 herein during the continuance of this Agreement. You agree that you own no right, title or interest in or to the Materials or any of the intellectual property rights therein. You shall have no rights hereunder other than the license as provided for above in Section 2. No right, license or interest to any trademark, trade name, service mark or other branding ("Marks") of WILEY or its licensors is granted hereunder, and you agree that you shall not assert any such right, license or interest with respect thereto.

5. WILEY DOES NOT MAKE ANY WARRANTY OR REPRESENTATION OF ANY KIND TO YOU OR ANY THIRD PARTY, EXPRESS, IMPLIED OR STATUTORY, WITH RESPECT TO THE MATERIALS OR THE ACCURACY OF ANY INFORMATION CONTAINED IN THE MATERIALS, INCLUDING, WITHOUT LIMITATION, ANY IMPLIED WARRANTY OF MERCHANTABILITY, ACCURACY, SATISFACTORY QUALITY, FITNESS FOR A PARTICULAR PURPOSE, USABILITY, INTEGRATION OR NON-INFRINGEMENT AND ALL SUCH WARRANTIES ARE HEREBY EXCLUDED BY WILEY AND WAIVED BY YOU.

6. WILEY shall have the right to terminate this Agreement immediately upon breach of this Agreement by you.

7. You shall indemnify, defend and hold harmless WILEY, its directors, officers, agents and employees, from and against any actual or threatened claims, demands, causes of action or proceedings arising from any breach of this Agreement by you.

8. IN NO EVENT SHALL WILEY BE LIABLE TO YOU OR ANY OTHER PARTY OR ANY OTHER PERSON OR ENTITY FOR ANY SPECIAL, CONSEQUENTIAL, INCIDENTAL, INDIRECT, EXEMPLARY OR PUNITIVE DAMAGES, HOWEVER CAUSED, ARISING OUT OF OR IN CONNECTION WITH THE DOWNLOADING, PROVISIONING, VIEWING OR USE OF THE MATERIALS REGARDLESS OF THE FORM OF ACTION, WHETHER FOR BREACH OF CONTRACT, BREACH OF WARRANTY, TORT, NEGLIGENCE, INFRINGEMENT OR OTHERWISE (INCLUDING, WITHOUT LIMITATION, DAMAGES BASED ON LOSS OF PROFITS, DATA, FILES, USE, BUSINESS OPPORTUNITY OR CLAIMS OF THIRD PARTIES), AND WHETHER OR NOT THE PARTY HAS BEEN ADVISED OF THE POSSIBILITY OF SUCH DAMAGES. THIS LIMITATION SHALL APPLY NOTWITHSTANDING ANY FAILURE OF ESSENTIAL PURPOSE OF ANY LIMITED REMEDY PROVIDED HEREIN.

9. Should any provision of this Agreement be held by a court of competent jurisdiction to be illegal, invalid, or unenforceable, that provision shall be deemed amended to achieve as nearly

as possible the same economic effect as the original provision, and the legality, validity and enforceability of the remaining provisions of this Agreement shall not be affected or impaired thereby.

10. The failure of either party to enforce any term or condition of this Agreement shall not constitute a waiver of either party's right to enforce each and every term and condition of this Agreement. No breach under this agreement shall be deemed waived or excused by either party unless such waiver or consent is in writing signed by the party granting such waiver or consent. The waiver by or consent of a party to a breach of any provision of this Agreement shall not operate or be construed as a waiver of or consent to any other or subsequent breach by such other party.

11. This Agreement may not be assigned (including by operation of law or otherwise) by you without WILEY's prior written consent.

12. These terms and conditions together with CCC's Billing and Payment terms and conditions (which are incorporated herein) form the entire agreement between you and WILEY concerning this licensing transaction and (in the absence of fraud) supersedes all prior agreements and representations of the parties, oral or written. This Agreement may not be amended except in a writing signed by both parties. This Agreement shall be binding upon and inure to the benefit of the parties' successors, legal representatives, and authorized assigns.

13. In the event of any conflict between your obligations established by these terms and conditions and those established by CCC's Billing and Payment terms and conditions, these terms and conditions shall prevail.

14. WILEY expressly reserves all rights not specifically granted in the combination of (i) the license details provided by you and accepted in the course of this licensing transaction, (ii) these terms and conditions and (iii) CCC's Billing and Payment terms and conditions.

15. This Agreement shall be governed by and construed in accordance with the laws of England and you agree to submit to the exclusive jurisdiction of the English courts.

BY CLICKING ON THE "I ACCEPT" BUTTON, YOU ACKNOWLEDGE THAT YOU HAVE READ AND FULLY UNDERSTAND EACH OF THE SECTIONS OF AND PROVISIONS SET FORTH IN THIS AGREEMENT AND THAT YOU ARE IN AGREEMENT WITH AND ARE WILLING TO ACCEPT ALL OF YOUR OBLIGATIONS AS SET FORTH IN THIS AGREEMENT.

V1.2

Gratis licenses (referencing $0 in the Total field) are free. Please retain this printable license for your reference. No payment is required.

If you would like to pay for this license now, please remit this license along with your payment made payable to "COPYRIGHT CLEARANCE CENTER" otherwise you will be invoiced within 30 days of the license date. Payment should be in the form of a check or money order referencing your account number and this license number 2323370380849. If you would prefer to pay for this license by credit card, please go to http://www.copyright.com/creditcard to download our credit card payment authorization form.

Make Payment To:
Copyright Clearance Center
Dept 001
P.O. Box 843006
Boston, MA 02284-3006

If you find copyrighted material related to this license will not be used and wish to cancel, please contact us referencing this license number 2323370380849 and noting the reason for cancellation.

Questions? customercare@copyright.com or +1-877-622-5543 (toll free in the US) or +1-978-646-2777.

WSPC Permission

Dear Andrew Cott

Thanks for contacting us regarding the attached permission request. We will be pleased to grant you the permission provided that full acknowledgment given to the original source. Kindly be noted that permission is granted on a non-exclusive and one-time basis only.

Warm regards

Tu Ning

From: ntu@wspc.org.sg

Original Message:

Andrew Cott
1605 Humboldt
Manhattan, KS 66502

December 8, 2009

Dear Sir or Madam:

I am writing to request permission to reuse a figure from an article published by your organization. I request to use this figure for the purpose of my Master's Report at Kansas State University. The article, its authors, and the figure I request permission to use is:

Grierson, D., & Gong, Y., & Xu, L. (2006). Optimal performance-based seismic design using modal pushover analysis. Journal of Earthquake Engineering, Vol 10, No 1. Figure 6, page 90.

I appreciate your time in considering my request. For comments or clarification, please respond to this email address or call at 785.458.2396. Again, I appreciate your time and effort in helping me to appropriately illustrate my Master's Report.

Sincerely,

Andrew Cott